5-2000

Joint effects of larval dispersal, population regulation, marine reserve design, and exploitation on production and recruitment in the Caribbean spiny lobster

WT Stockhausen
Virginia Institute of Marine Science

Rom Lipcius
VIMS

BM Hickey

BULLETIN OF MARINE SCIENCE, 66(3): 957–990, 2000

JOINT EFFECTS OF LARVAL DISPERSAL, POPULATION REGULATION, MARINE RESERVE DESIGN, AND EXPLOITATION ON PRODUCTION AND RECRUITMENT IN THE CARIBBEAN SPINY LOBSTER

William T. Stockhausen, Romuald N. Lipcius and Barbara M. Hickey

ABSTRACT

A spatially explicit population-dynamics model for the Caribbean spiny lobster (*Panulirus argus*) in Exuma Sound, Bahamas, was used to investigate the joint effects of marine reserve design and larval dispersal via hydrodynamic currents on an exploited benthic invertebrate. The effects of three hydrodynamic scenarios (one diffusion-only and two advection-diffusion cases), one exploitation level, and 28 reserve configurations (7 sizes × 4 locations) on catch and larval production were simulated. The diffusion-only scenario represented the condition in which settlement did not vary substantially over broad spatial scales; in contrast, the advection-diffusion scenarios represented realistic hydrodynamic patterns and introduced broad spatial variation. Both advection-diffusion scenarios were based on empirical measurements of near-surface flow in Exuma Sound. Catches were sensitive to interactions between reserve configuration and pattern of larval dispersal. A given reserve configuration led to enhancement or decline in catch, depending on the hydrodynamic scenario, reserve size, and reserve location. Larval production increased linearly with reserve size, when size was expressed as the population fraction initially protected by the reserve, but when reserve size was expressed as the fraction of coastline protected, larval production decreased for some reserve configurations under the two advection-diffusion hydrodynamic scenarios. Use of a simple reserve-design rule (e.g., protect 20% of a coast) would, in the latter cases, lead to a false sense of security, thereby endangering—not protecting—exploited stocks. The optimal design of marine reserves therefore requires attention to the joint effects of larval dispersal, reserve location, and reserve size on fishery yield and recruitment.

Most benthic invertebrates and reef-associated fish undergo a dispersive, planktonic larval stage before settlement and metamorphosis into the juvenile and adult stages (Thorson, 1950; Mileikovsky, 1971; Roughgarden et al., 1988; Leis, 1991). In some species, settlement may be decoupled from adult abundance at local spatial scales if hydrodynamic conditions or larval behavior do not promote local retention (Fogarty, 1998; Lipcius et al., 1997). Similarly, spatial and temporal variability in postsettlement mortality or secondary dispersal by juveniles and adults may decouple spatial patterns of adult abundance from those of settlement (Jones, 1991). Spatial patterns of settlement and adult abundance may therefore be functionally related in a complex fashion.

The manner in which biotic or environmental factors control spatial patterns of abundance at different life-history stages may have profound implications for the management of exploited benthic marine species, particularly if patterns of exploitation are themselves spatially structured. The use of marine reserves (no-take areas or harvest refugia, sensu Dugan and Davis, 1993), an increasingly popular strategy for fisheries management, imposes explicit constraints on spatial patterns of exploitation, but the effects of interactions between natural factors controlling abundance and spatially segregated exploitation are not well understood.

Marine reserves can be viable tools for sustainable fisheries management (Roberts and Polunin, 1991; Dugan and Davis, 1993) that potentially enhance fisheries through two mechanisms: local migration (surplus adults emigrate from reserves to adjacent areas and become vulnerable to the fishery) and enhanced recruitment (larval or postlarval supply, settlement, and recruitment to the fishery are increased at regional scales by surplus reproductive output from reserves). These mechanisms involve dramatically different spatial scales (local and regional) and processes (e.g., density-dependent migration and density-independent dispersal). The effectiveness of reserves for fisheries enhancement will therefore depend on the interaction between reserve design (i.e., size, shape, and location) and the relative importance of local and regional processes in controlling spatial patterns of population abundance.

Numerous field studies of reserve function have demonstrated enhanced fisheries production of temperate and tropical reef fish (e.g., Alcala and Russ, 1990; Russ and Alcala, 1996) and invertebrates (e.g., Davis and Dodrill, 1980, 1989; Gitschlag, 1986; Yamasaki and Kuwahara, 1990) through local emigration. In contrast, field demonstration of enhancement of recruitment by reserves remains elusive because of the difficulties in experimenting with the processes that control temporal and spatial variability in larval supply and recruitment success (Doherty, 1991; Doherty and Fowler, 1994; Man et al., 1995). Much of the effort dealing with the effects of reserves on recruitment and fisheries production therefore involves modeling efforts (Polacheck, 1990; Die and Watson, 1992; DeMartini, 1993; Quinn et al., 1993; Attwood and Bennett, 1995; Man et al., 1995; Holland and Brazee, 1996; Sladek Nowlis and Roberts, 1997, 1999; Lauck et al., 1998; Hastings and Botsford, 1999; see also Guénette et al., 1998).

Previous modeling studies evaluating the effectiveness of marine reserves in enhancing fishery yield and recruitment reached mixed conclusions. In two-habitat (reserve and exploited) patch cohort models with reduced mortality within the reserve, increasing reserve size increased spawning-stock biomass per recruit (SSB/R), whereas yield per recruit (Y/R) was generally reduced in temperate (Polacheck, 1990) and coral-reef (DeMartini, 1993) fish. Increasing transfer rates of postsettlement individuals between reserve and fished areas, as well as increasing fishing pressure outside the reserve, diminished the effects of increased reserve size, but the positive effect on SSB/R from increased reserve size generally outweighed the negative effect on Y/R when transfer rates were independent of density (Polacheck, 1990; DeMartini, 1993). Conversely, density-dependent transfer rates negated enhancement of SSB/R; reserves were unlikely to augment SSB/R in heavily exploited species without complementary regulation of effort and size composition in exploited areas (DeMartini, 1993).

Die and Watson (1992) used a two-patch model to address the utility of inshore marine reserves for enhancing the Australian penaeid shrimp fishery. Recruitment to the population occurred only in the closed area; migration from closed to open areas made animals vulnerable to capture by the fishery. Averaged over ranges of fishing and natural mortality rates, mean changes in Y/R for the three migration rates considered were negative at all reserve sizes. Y/R declined fastest with reserve size for the slowest migration rate. Conversely, mean value per recruit (V/R) initially increased with reserve size for all three migration rates; ultimately, it decreased with reserve size for the lower two migration rates. In all cases, the mean number of eggs per recruit increased with reserve size.

In a two-patch logistic model, population collapse of the red sea urchin, *Strongylocentrotus franciscanus*, was prevented by a marine reserve, even at high levels

of exploitation when the species was also subject to Allee effects in reproduction or recruitment (Quinn et al., 1993). A more detailed age-structured, spatially explicit model incorporating larval dispersal through simple diffusion produced similar results. Multiple small reserves spaced closer than the average distance of larval dispersal were more effective than larger, but fewer and more distantly spaced, reserves in sustaining the exploited population (Quinn et al., 1993).

Using a spatially explicit, age-structured model, Attwood and Bennett (1995) varied recruitment and dispersal according to the life-history characteristics of three sympatric surf-zone fish species favored by shore anglers in South Africa. Recruitment was assumed to be independent of local abundance for one species (white steenbras, *Lithognathus lithognathus*), whereas recruitment-spawner biomass functions were used to compute local settlement rates for the other two (galjoen, *Dichistius capensis*, and blacktail, *Diplodus sargus capensis*). Tag returns indicated little or no postsettlement movement for blacktail, so dispersal was assumed to be via passive larval drift. Transfer rates for larval blacktail between adjacent model cells were assumed to be by simple diffusion. Postsettlement transfer rates between model cells for white steenbras and galjoen were estimated from tag return data. The impact of reserve size and spacing on Y/R or yield (Y) was evaluated differently for different species. Because recruitment was assumed constant for white steenbras, model results for this species were evaluated in terms of Y/R and SSB/R, whereas results for galjoen and blacktail were evaluated in terms of Y alone. For white steenbras, SSB/R increased with reserve size, whereas Y/R decreased (Attwood and Bennett, 1995). For a given reserve size, SSB/R decreased as reserve spacing increased, whereas Y/R increased. For galjoen, Y increased dramatically as reserve size increased (Attwood and Bennett, 1995). For blacktail, closely spaced reserves optimized yield (Attwood and Bennett, 1995). No results regarding spawning stock were reported for galjoen or blacktail.

In a metapopulation model for tropical reef fish, the ratio of extinction rate to colonization rate in exploited patches was the key parameter determining optimal reserve size, defined as the fraction of habitat patches protected (Man et al., 1995). When fishing pressure was low or colonization rate high, maximum sustained yield (MSY) was obtained without reserves; as fishing pressure increased or colonization rate decreased, the optimal fraction of patches set aside as reserves increased asymptotically to 0.5. For a given ratio, MSY was obtained when half of all patches (reserve + exploited) were occupied at equilibrium.

Using a two-patch model, Holland and Brazee (1996) examined the utility of marine reserves for fisheries management of the Gulf of Mexico red snapper from an economic perspective. Their model incorporated a stock-recruit relationship and the concept of the present value of harvest (PVH), which uses discounted values of future harvests over a given time horizon, to determine optimal reserve size. Increasing discount rates resulted in smaller optimal reserves sizes. With a 60-yr PVH time horizon, no combination of reserve size and fishing effort performed better than the MSY fishing effort (0.75) with no reserve. When fishing effort was slightly larger than MSY (0.75–1.0), optimal reserve sizes were negligibly small, but when effort was much larger than MSY (1.5–2.0), optimal reserve sizes ranged from 15 to 20% and resulted in PVHs 4–8% higher than those in the absence of a reserve.

In a two-patch model incorporating stochastic exploitation rates, the probability that stock abundance remained >60% of carrying capacity after 20 yrs of exploitation at a

given mean rate was a function of the reserve area (relative to total area) and the coefficient of variation (cv) in the harvest rate (Lauck et al., 1998). For moderate cv's, the chance of success declined rapidly as reserve size decreased below 70%. For higher cv's, the probability of success was <1 even when harvested areas were very small. Reserves allowed higher mean harvest rates, with consequent higher catches, while still protecting the stock.

Sladek Nowlis and Roberts (1997, 1999) used two-patch models for several exploited coral-reef species to examine short- and long-term effects of reserve establishment on fishery yields. Reserves were only effective in increasing fishery yields when fisheries were overexploited in the absence of a reserve. For a fixed reserve size, greatly overexploited fisheries recovered faster than more lightly exploited ones from initial losses associated with reserve establishment (Sladek Nowlis and Roberts, 1997). For a fixed fishing intensity, larger reserves resulted in higher catches after 30 yrs (Sladek Nowlis and Roberts, 1997). Optimal reserve size (the size that produced the highest long-term yield for a given fishing intensity) increased with fishing intensity, and yields associated with optimal reserves were similarly high over a range of fishing intensities for most of the species considered (Sladek Nowlis and Roberts, 1999).

Finally, Hastings and Botsford (1999) demonstrated that a system of optimally sized marine reserves in a two-patch model could achieve maximum yields identical to that possible under allocation of a fixed fraction of a stock to a fishery—a more traditional management approach.

The principal mechanism determining spatial structure in these models is the spatial pattern of exploitation. A major assumption in many of these models (Polacheck, 1990; DeMartini, 1993; Attwood and Bennett, 1995; Man et al., 1995; Sladek Nowlis and Roberts 1997, 1999; Hastings and Botsford, 1999) is that larvae are so well mixed over the area the population occupies that relative recruitment to reserve and exploited areas is identical to the proportion of each relative to the total area. As a consequence, reserve function is evaluated in terms of reserve size and, possibly, spacing. However, hydrodynamic current patterns may play an important role in how a marine reserve functions (Carr and Reed, 1993). Through advective transport of larvae, hydrodynamic currents can impose spatial structure on settlement at regional scales for benthic species (Tremblay et al., 1994; Lipcius et al., 1997). Hydrodynamic conditions may thus modify patterns of connectivity among widely separated subpopulations. Consequently, the interaction between hydrodynamic currents (Lipcius et al., 1997; Fogarty, 1998) and the location of spawning stock may determine the optimal design of reserves for widely dispersing marine species (Carr and Reed, 1993; Roberts, 1997).

Reserve location may therefore be as important as size in determining reserve performance. Because previous empirical and theoretical studies have not addressed this issue, our primary objective is to model the joint effects of hydrodynamic current pattern (with concomitant larval dispersal) and marine reserve configuration (location and size) on reserve function for an exploited benthic invertebrate with a widely dispersing larval phase. Specifically, we wish to determine (1) whether reserves of similar size but different locations function equivalently for a given pattern of larval dispersal, (2) whether reserves of similar size and location function equivalently under different patterns of larval dispersal, and (3) whether 'optimal' reserve size and location are similar under different patterns of larval dispersal. The model we use integrates the effects of reserve size and location, larval transport via oceanic currents, postsettlement dispersal and mor-

tality, and adult spawning on the population dynamics of an exploited benthic invertebrate with a complex life history. Model parameters are based on the life history of the Caribbean spiny lobster, *Panulirus argus*, in Exuma Sound, Bahamas. The use of marine reserves to enhance spiny lobster fisheries is a topic of interest (see, e.g., Davis and Dodrill, 1980; Childress, 1997; Acosta, 1999), so our choice of model system is applicable as a heuristic examination for both spiny lobster and other exploited species with complex life histories.

Methods

In this study, we focus on interactions between patterns of larval dispersal (and subsequent juvenile recruitment) and reserve configuration (i.e., size and location). As part of recent (Lipcius et al., 1997) and continuing work with Caribbean spiny lobster, *P. argus*, in Exuma Sound, Bahamas, we have developed a preliminary population-dynamics model for this system that encompasses demographic processes during all life-history stages and 'closes the larval loop', coupling postsettlement benthic population dynamics, adult spawning, and planktonic larval dispersal (Gaines and Lafferty, 1995; Eckman, 1996). The model is preliminary, however; we use it here as a heuristic tool to explore the impact of hypothetical reserves on a hypothetical population described by the model. Our model extends the two-dimensional spatially structured, coupled planktonic/benthic population model of Possingham and Roughgarden (1990) to include multiple pelagic and benthic life-history stages, curvilinear coastal geometry and complex current patterns, and postsettlement dispersal. For this study, we also incorporated spatial variation in fishing mortality to accommodate reserve–exploited area distinctions. We used the model to simulate the population dynamics of spiny lobster in Exuma Sound, with concomitant fishery yields, for a combination of different hydrodynamic current patterns, exploitation rates, and marine-reserve configurations.

Life History of *Panulirus argus*.—The Caribbean spiny lobster is a macrobenthic invertebrate with widely dispersing larvae and supports commercially valuable fisheries in Florida and the Caribbean (Bohnsack et al., 1994). Like other spiny lobster species, *P. argus* exhibits five distinct life-history stages: egg, phyllosoma larva, puerulus postlarva, benthic juvenile, and adult (Phillips et al., 1980; Lipcius and Cobb, 1994; Lipcius and Eggleston, in press). The larval and postlarval stages constitute the pelagic phase of the spiny lobster life history. Phyllosome larvae are released from eggs hatched on the seaward fringes of coral reefs. Subsequently, the larvae lead an oceanic planktonic existence during which they progress through approximately 11 larval stages, while growing from less than 1 mm to 12 mm carapace length (CL; Lewis, 1951; Lyons, 1980). After 4–9 mo in the plankton, surviving larvae undergo radical metamorphosis to the transparent, nonfeeding puerulus postlarval stage, which is about 6 mm CL (Lewis, 1951; Lewis et al., 1952). Postlarvae are vigorous swimmers and actively migrate into coastal waters, where they subsequently invade shallow inshore areas during nighttime flood tides associated with the new moon (Little, 1977; Calinski and Lyons, 1983; Herrnkind and Butler, 1986; Eggleston et al., 1998). The pueruli settle to the benthos in structurally complex habitats such as clumps of red macroalgae (*Laurencia* spp.) or among mangrove roots (Marx and Herrnkind, 1985; Butler and Herrnkind, 1992). Within several days of settlement, surviving postlarvae acquire pigmentation and metamorphose into the first juvenile benthic instar.

On the basis of ontogenetic habitat shifts during the benthic juvenile stage, investigators agree in dividing this stage into three substages: algal phase, postalgal phase, and subadult (Marx and Herrnkind, 1985; Herrnkind and Lipcius, 1989). Algal-phase juveniles use the structurally complex settlement habitat for both shelter and foraging (Marx and Herrnkind, 1985). They undergo a solitary existence, increasing in size through a series of molts from 6 to 25 mm CL over a period of several months. After reaching 15 mm CL, algal-phase lobsters begin to use crevices, tube sponges, and octocorals for shelter (Marx and Herrnkind, 1985; Smith and Herrnkind, 1992; Forcucci et al.,

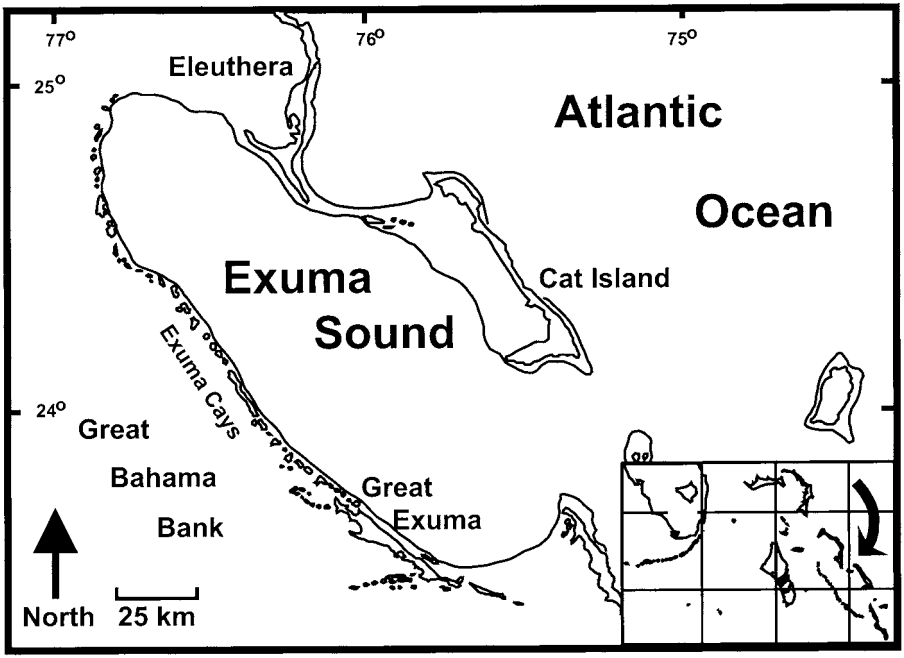

Figure 1. Exuma Sound, Bahamas.

1994; Butler and Herrnkind, 1997). Postalgal-phase juveniles (15–45 mm CL) are fairly site-attached, staying within several meters of their daytime shelter (Herrnkind and Butler, 1986). At night they emerge from these daytime shelters to forage for small molluscs and crustaceans in neighboring habitats (Andree, 1981; Herrnkind et al., 1994). The gregarious behavior typical of older juveniles and adults is first exhibited during this stage (Berrill, 1975).

Subadults (>45 mm CL) are nomadic and forage widely in hard-bottom habitats and sea-grass/algal meadows (Herrnkind, 1980, 1983). As they approach sexual maturity (~76 mm CL), larger juveniles migrate seaward toward offshore reefs (Herrnkind and Lipcius, 1989).

Adults (>75–80 mm CL) are gregarious as well, dwelling in dens of 20 or more lobsters (Herrnkind and Lipcius, 1989). Adult sex ratios are size dependent; males tend to be larger than females, reflecting greater female reproductive investment and differences in molting patterns (Lipcius and Herrnkind, 1987; Herrnkind and Lipcius, 1989). In Exuma Sound, peak reproductive activity occurs in spring (Herrnkind and Lipcius, 1989).

SITE.—Exuma Sound is a deep (>1000 m), semienclosed basin in the central Bahamas, surrounded by the Exuma Cays and the Great Bahama Bank to the north and west, by Eleuthera and Cat Island to the east, and by Long Island to the south (Fig. 1). Approximately 200 km northwest to southeast and 75 km at its widest, the sound has two connections to the Atlantic Ocean: a deep (2000 m depth) gap 50 km wide between Long and Cat islands and a shallow sill (15–30 m depth) 27 km wide between Eleuthera and Cat Island. Except for these openings, Exuma Sound is bordered by either low islands or shallow carbonate bank. Exuma Sound provides habitats for spiny lobster on all sides, making the system particularly well suited for analyses of the relationships between meteorology, oceanography, recruitment, and population dynamics.

Circulation in Exuma Sound appears to be dominated by large-scale, vigorous gyres extending to depths as great as 200 m (Fig. 2; Hickey, 1995). Water exchange with the open ocean occurs regularly, and exchange with the shallow banks also occurs through dense, high-salinity intrusions. Wind forcing plays an important role in the circulation by influencing the current structure in the

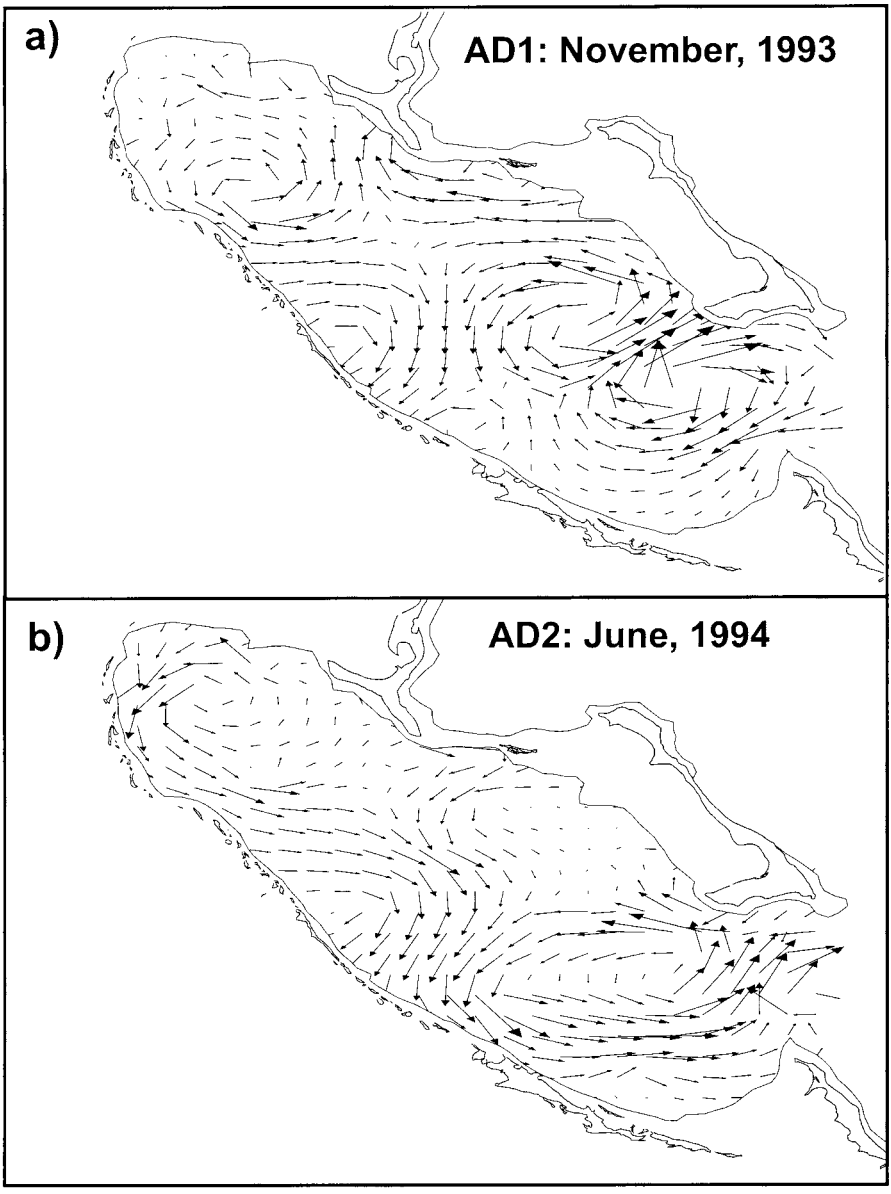

Figure 2. Near-surface geostrophic current patterns (relative to 500 db) derived from CTD data collected during cruises in Exuma Sound (Hickey, 1995): (A) November 1993, (B) June 1994.

upper 15 m of the water column. Mesoscale features with associated fronts are superimposed on a general northwestward drift and cause convergence and preferred pathways through the sound (Colin, 1995; Hickey, 1995). Although the gyres appear to be semipermanent features in the sound, they may oscillate seasonally (Fig. 2); substantial variability in near-surface currents exists at 10–30-d time scales (Hickey, 1995).

Model Description.—The full spiny lobster population dynamics model is composed of three coupled submodels: the pelagic model, the benthic model, and the reproduction model. The spatial

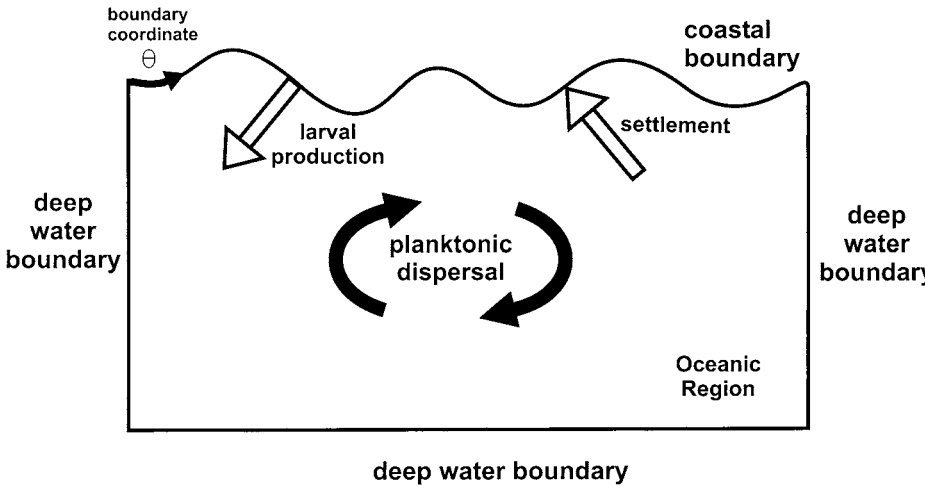

Figure 3. Conceptualized geometry for the complex life-history model.

domain for the model consists of a two-dimensional (horizontal), oceanic region with its one-dimensional boundary, the latter encompassing both shallow coastal regions, where settlement can occur, and deep-water regions, where it cannot (Fig. 3).

The pelagic model tracks changes in age-specific, spatially structured density of larvae, L_0, and postlarvae, L_1, within the oceanic region due to (1) hatching of larvae following adult reproduction along the coast, (2) aging, (3) mortality, (4) horizontal dispersal via two-dimensional advective currents and turbulent diffusion, (5) metamorphosis from larval stage to postlarval stage, and (6) settlement in shallow coastal regions on the spatial boundary. We regard the pelagic densities as continuous functions of space (x, y), time (t), and age within stage (a), so we developed a set of coupled reaction-advection-diffusion partial differential equations (PDEs) with associated boundary conditions to describe the temporal and spatial dynamics of the planktonic stages (see Appendix for details). Seasonal spawning and subsequent larval production within the shallow coastal

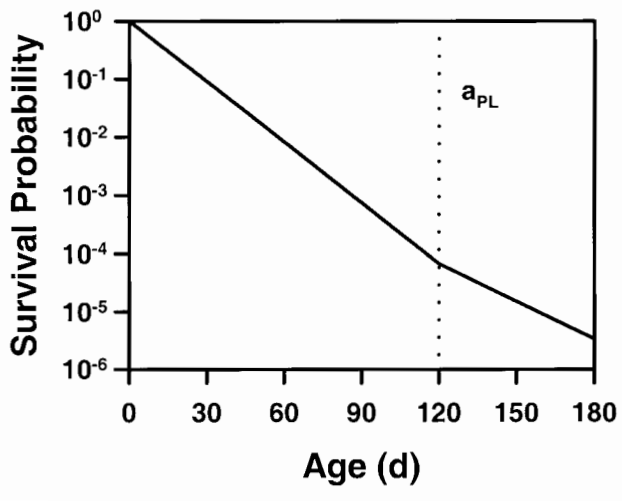

Figure 4. Probability of survival vs age for larvae and postlarvae using the baseline parameters for the pelagic submodel (Table 1).

Table 1. Parameters for the Caribbean spiny lobster pelagic life-history stage model.

Parameter	Value	Units
Age at metamorphosis to postlarva, a_{pl}	120	d
Maximum postlarval age	60	d
Mortality coefficients		
μ_0	0.08	d^{-1}
μ_1	0.05	d^{-1}
Postlarval swimming speed		
offshore	0.5	km d^{-1}
coastal	2.0	km d^{-1}
Turbulent diffusivity, K	0.864	km^2 d^{-1}
Boundary leakage function		
coastal, *larval stage*	0.0	(none)
deep-water, *larval stage*	0.5	(none)
coastal, *postlarval stage*	1.0	(none)
deep-water, *postlarval stage*	0.0	(none)

regions on the spatial boundary determine the local influx of age-0 planktonic larvae into the oceanic region; larvae are subsequently transported from their hatching grounds by spatially variable advective currents and dispersed through turbulent diffusion. For this study, larvae were subjected to a constant mortality rate, independent of density, location, age, and time of year (Table 1). Metamorphosis from the larval to the postlarval stage occurs as an instantaneous process at an age of 120 d. This value represents the lower end of probable larval duration (4–6 mo in Exuma Sound, up to 9 mo at extremes of the geographic range; Lipcius and Eggleston, in press), but the combination of mortality rate and stage duration means that less than 0.01% of larvae hatched survive until metamorphosis to postlarvae (Fig. 4).

Postlarvae are strong swimmers and actively migrate to settlement areas (Little, 1977; Calinski and Lyons, 1983; Herrnkind and Butler, 1986). In shallow areas, postlarvae attach to structures or bury themselves in sand (Calinski and Lyons, 1983), a behavior that may enhance onshore transport near the coast if synchronized with adverse tidal flows. We therefore added an active, deterministic component to postlarval dispersal in addition to advection by mean currents and dispersal through turbulent diffusion. We also assumed that postlarvae orient toward the nearest coastline (by means of some unspecified environmental cue, possibly chemical) so that the local direction of active migration was toward the nearest coastal region, while the effective speed of migration was higher near the coast than further offshore. The local age-integrated flux of postlarvae across the coastal boundary determines local settlement rates. Prior to settlement, postlarvae are subjected to a constant mortality rate (Table 1) such that approximately 10% survive after 30 d in the pelagic zone (Fig. 4). Postlarvae are a nonfeeding stage with an estimated duration of a few weeks (Booth and Phillips, 1994; Butler and Herrnkind, 1997); postlarvae that had not settled within 60 d of larval metamorphosis were therefore regarded as dead.

The benthic model tracks changes in the size-specific, spatially structured density along the coast for algal phase (s_1), postalgal phase (s_2), subadult (s_3), and adult (male, s_4; female, s_5) life-history stages due to (1) settlement, (2) mortality, (3) growth within a life-history stage, (4) transition between successive life-history stages, and (5) alongshore dispersal. Like pelagic densities, the stage-specific benthic densities are continuous functions—but of size (z), rather than age; of space (θ, position along the one-dimensional spatial boundary which includes shallow, coastal and unsuitable, deep-water benthic habitats); and of time (t). Again, we used a set of coupled PDEs with associated boundary conditions to describe the population dynamics of the benthic life-history stages (see Appendix for details). Local settlement provides the population 'source' term for the benthic model. 'Settled' postlarvae metamorphose into algal-phase benthic juveniles in the 6–7-

Table 2. Parameters for the Caribbean spiny lobster benthic life-history stage model.

Parameter	Algal phase	Postalgal phase	Subadult	Adult male	Adult female	Units
Habitat index, ψ_i						
c_i	5,000	5,000	2,500	1,000	1,000	No. km^{-1}
Stage size limits						
z_i^{min}–z_i^{max}	6–25	20–45	40–80	75–150	75–150	mm CL
Growth, g_i						
α_i	0.009	0.002	0.002	0.0009	0.0009	d^{-1}
β_i	50	150	150	150	150	mm CL
Natural mortality, μ_i^n						
c_{i1}	0.01	0.005	0.0025	0.0009	0.0009	d^{-1}
c_{i2}	2	2	2	2	2	(none)
c_{i3}	1.0	1.0	1.0	1.0	1.0	(none)
Dispersal, J_i						
c_{i1}	0	0	0.05	0.01	0.01	km^2 d^{-1}
c_{i2}	0	0	5	5	5	(none)
c_{i3}	0	0	1	1	1	(none)
Life-history stage transition rates, τ_{ij}						
$j \rightarrow i$	1 $\rightarrow$2	2 $\rightarrow$3	3 $\rightarrow$4	3 $\rightarrow$5		
c_{ij1}	0.05	0.025	0.02	0.02		d^{-1}
c_{ij2}	0.5	0.5	0.5	0.5		mm^{-1}

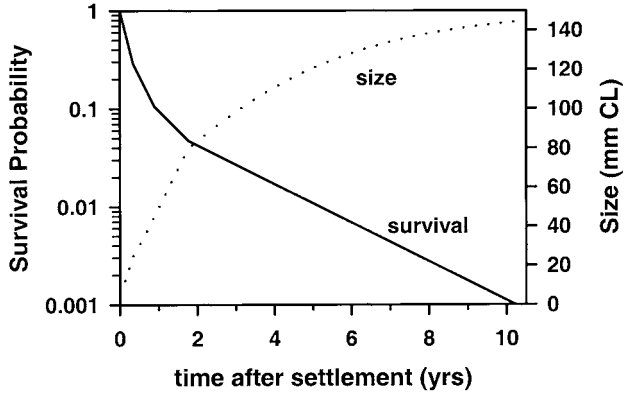

Figure 5. Probability of survival and size vs age for benthic life-history stages using the baseline parameters for the benthic submodel (Table 2). Density dependence is ignored.

mm CL size range, typical of first benthic instars in Exuma Sound (Eggleston et al., 1998). We decomposed total mortality rates into a sum of 'natural' and fishing mortalities. For this study, natural mortality rates were functions of local stage-specific densities but did not otherwise depend on size, location, or time. Availability of appropriately sized shelter appears to be a key factor in regulating local abundance of benthic life-history stages (Butler and Herrnkind, 1997; Lipcius and Eggleston, in press) and probably results in density-vague (Strong, 1984) mortality rates. We used piece-wise linear functions to describe density-dependent mortality rates—constant at low densities but increasing at high densities—for all benthic life-history stages (Table 2). When density is low, approximately 4% of settlers survive 2 yrs (Fig. 5). Local fishing mortality rates were stage-specific, size-structured, seasonal, and spatially explicit (see below). Although individual spiny lobsters increase in size through discrete molting events, we described growth as a continuous process because molting is not synchronous and the model deals with distributions rather than individuals (Botsford, 1985). We used a simple Gompertz-type growth function (see Appendix) with density-independent parameters to describe growth rates within a stage. Selected parameter values (Table 2) result in reasonable postsettlement growth histories (Fig. 5). Size ranges for subsequent life-history stages overlap, and transition from one benthic stage to the next sometimes occurs without growth; transition rates from the earlier stage increase with size within this range of overlap. After reaching maturity, males exhibit higher size-specific growth rates than females, reflecting the greater metabolic investment in reproduction by females (Lipcius, 1985), so the model includes both male and female adult stages. For this study, however, males and females are treated identically. Although subadult spiny lobsters in other areas of the Caribbean engage in (sometimes spectacular) seasonal migrations (Kanciruk and Herrnkind, 1978; Herrnkind, 1980, 1983), such activity has not been observed in Exuma Sound, where alongshore movements are nomadic (Herrnkind and Lipcius, 1989). We therefore described postsettlement dispersal along the coast as a density-dependent diffusion process; we did not include deterministic movement (i.e., an advective component) such as seasonal migrations.

The reproduction model tracks temporal and spatial variation in spawning and subsequent larval production along the coast, incorporating spawning seasons, size-specific fecundity, and size-specific adult female density (see Appendix for details). Larval production (i.e., spawning and hatching) begins in the late winter, peaks in the spring, and ends in the summer. We used a truncated normal distribution to approximate seasonal spawning rates (Table 3, Fig. 6A). We assumed females mature at 75 mm CL (Herrnkind and Lipcius, 1989; Lipcius et al., 1997). Because Lipcius et al. (1997) found no difference in spatial variation in fecundity in Exuma Sound, we described individual fecundity as an exponential function of adult size, but independent of local density, spatial location, and season (Fig. 6B). Parameters were based on a previous analysis of the fecun-

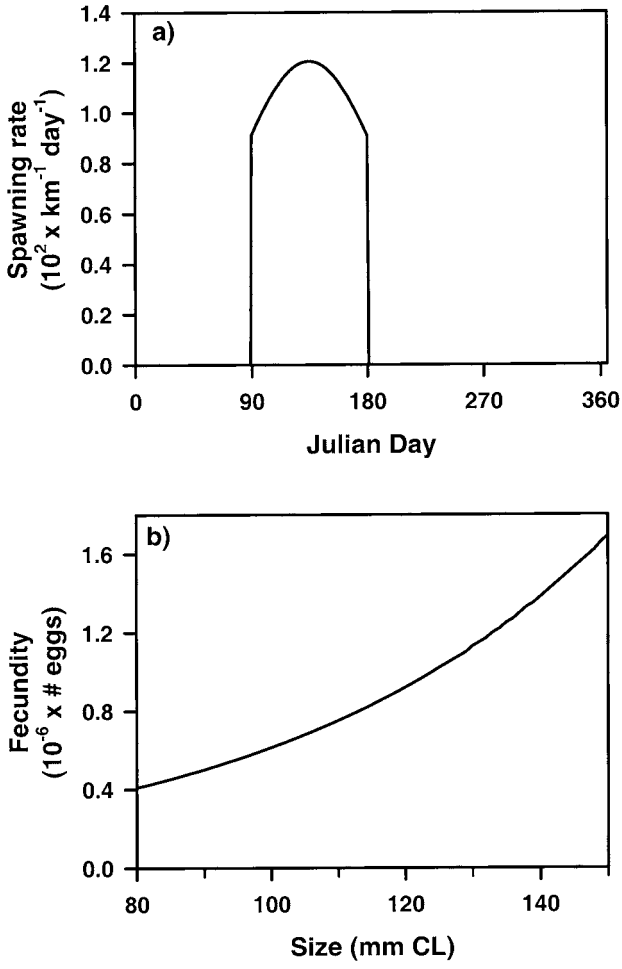

Figure 6. (A) Temporal spawning patterns and (B) size-specific fecundity using the baseline parameters for the adult spawning submodel (Table 3).

dity data used by Lipcius et al. (1997, see Table 3). The instantaneous rate of local larval production is the size-integrated product of size-specific fecundity and local adult density, weighted by the seasonally varying spawning rate. Coming full circle and "closing the larval loop" (Eckman, 1996), the local rate of larval production in coastal regions along the spatial boundary determines the flux of age-0 planktonic larvae into the oceanic region in the pelagic model.

Given the complexity of the model, it is not feasible to obtain analytical solutions to problems we wish to address, so we developed a numerical representation of the model based on standard techniques for integrating spatially structured, coupled PDEs. We also constructed a grid representation of Exuma Sound using 2.5- × 2.5-km^2 cells from a digitized map of Exuma Sound (Fig. 7). The grid consists of 1872 interior cells and 254 boundary sections. Of the 254 boundary sections, 21 contiguous sections constitute a deep-water boundary (52.5 km) representing the primary connection between Exuma Sound and the Atlantic at the southeast corner of the sound; the remaining sections constitute coastline available for settlement (582.5 km). Because there is no evidence for larval transport across the shallow sill between Cat Island and Eleuthera (Colin, 1995), we modeled this region as coastal habitat across which larvae do not disperse. We used a 1-d time step to integrate the model numerically for up to 50 model yrs.

Table 3. Baseline parameters for the Caribbean spiny lobster reproduction submodel.

Parameter	Value	Units
Maturity, m_i		
c_1	1	(none)
c_2	80	mm CL
Spawning rate, r_i		
$t^{start} - t^{end}$	90–180	Julian day
c_1	0.0115	d^{-1}
c_2	135	d
c_3	60	d
Fecundity, $\mathcal{F}_i$		
c_1	3.69×10^5	No. eggs
c_2	0.0203	mm^{-1}
c_3	75	mm CL

MODEL CASES.—To examine several different patterns of connectivity (via larval dispersal) in the study, we defined three hydrodynamic scenarios, consisting of two advection-diffusion cases (AD1 and AD2) and one diffusion-only case (D1), to incorporate the potential for differing patterns of spatial structure through larval dispersal. The diffusion-only scenario represented the condition in which settlement did not vary substantially over broad spatial scales, in contrast to the advection-diffusion scenarios, which represented realistic hydrodynamic transport conditions and broad spatial variation in the field. The advective currents for AD1 and AD2 were based on near-surface (5 m

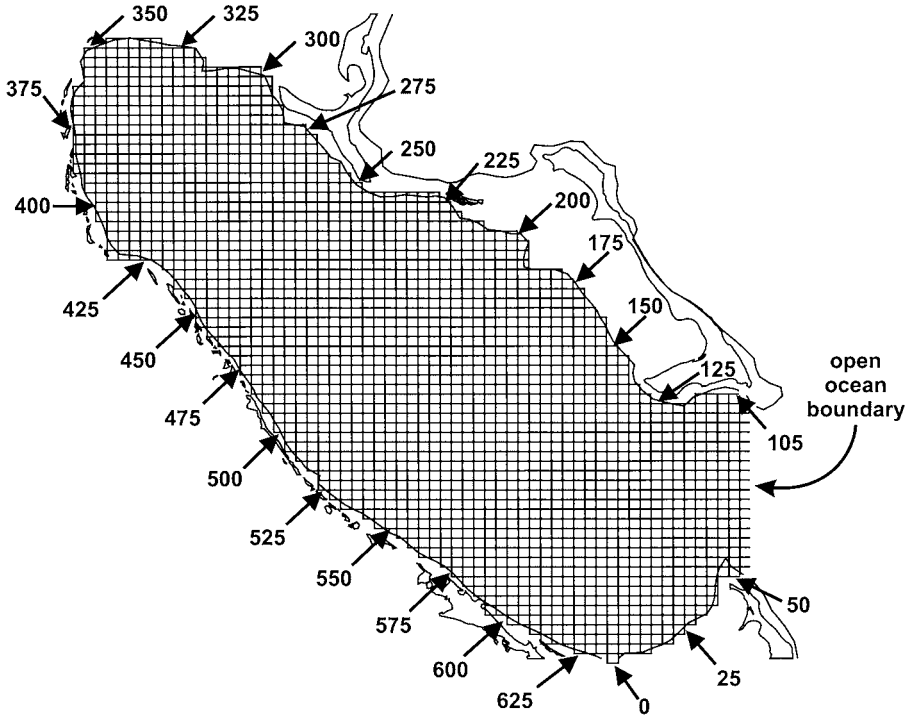

Figure 7. Computational model grid for Exuma Sound.

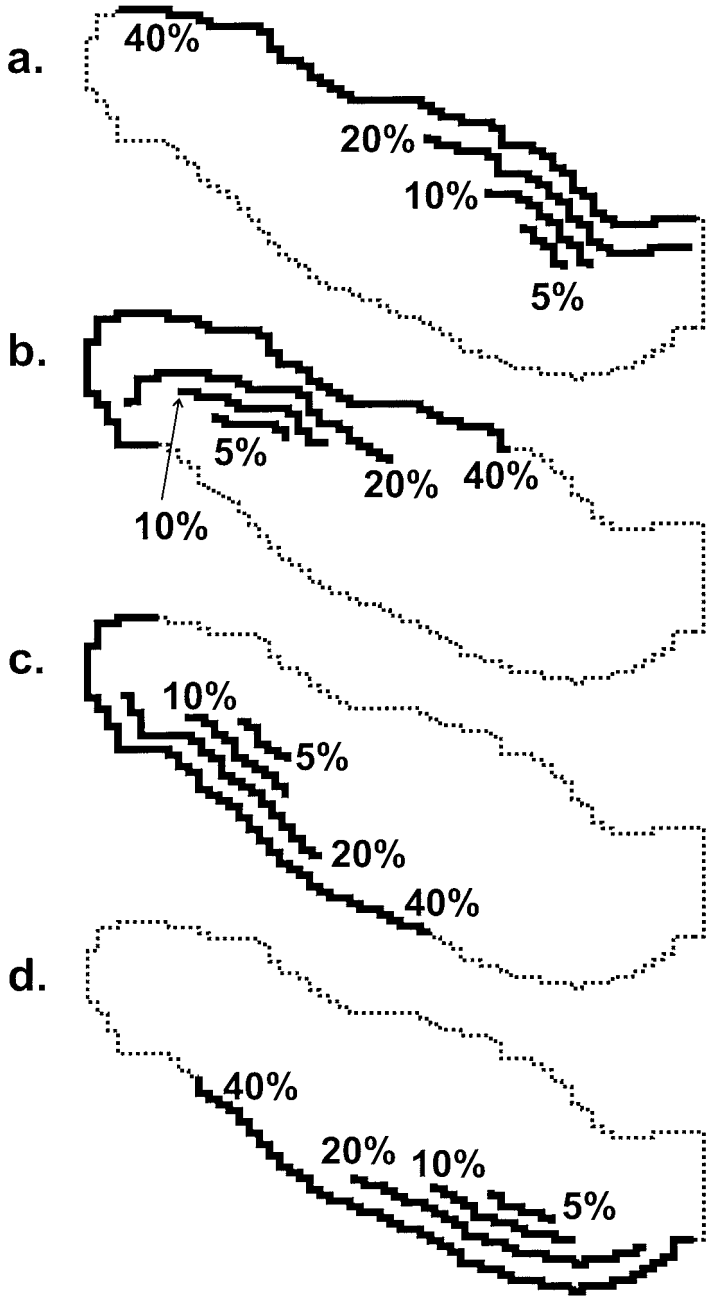

Figure 8. Marine reserve configurations used in simulations: (A) SE location, (B) NE location, (C) NW location, (D) SW location. Reserve sizes are given as percentage of the coastline. (Note: smaller sizes are shown offset from the coast; not all sizes used are illustrated).

depth) geostrophic currents in Exuma Sound derived from physical oceanographic data collected during November 1993 and June 1994 (Fig. 2), respectively. For both cases, the current pattern was fixed temporally. For D1, the advective currents were set to zero. Eddy-diffusion coefficients were identical for all three scenarios.

Model scenarios with no exploitation were created for each hydrodynamic current pattern; subsequently, the model was numerically integrated similarly for each case. Parameters reflecting mortality, growth, dispersal, and reproduction were identical for all three scenarios. Initial abundance patterns for each life-history stage were set to zero. Each model was started when larvae were 'injected' into the pelagic submodel at constant rates along the model boundary during the first three spawning seasons. After year 3, injection was discontinued, and the population continued to grow under its own dynamics, typically reaching a steady state after 25 model yrs. The numerical model was integrated for 50 model yrs. The complete model state was saved at the beginning of model year 30 and used to initialize subsequent model runs for scenarios including exploitation. Abundance patterns for each postsettlement stage, larval production, and postlarval settlement were saved at quarterly intervals during the final 10 model yrs.

We created a 'heavily exploited' case corresponding to each unexploited case using a nominal fishery mortality rate (F) of 1.0 yr^{-1}. We adjusted the instantaneous rate of fishing mortality for a fishing season that ran from Julian day 181 to Julian day 365. Effort was uniformly distributed along the coast, and only adults larger than 75 mm CL were vulnerable to the fishery. For each case, the model state from the corresponding unexploited case at the beginning of model year 30 was used to initialize the simulation run. The model was subsequently integrated numerically for 20 yrs. The complete model state was saved at the beginning of model year 40 and used to initialize subsequent model runs for marine reserve scenarios. Spatially explicit, instantaneous catch rates, $c(\theta,t)$, were calculated from the spatially explicit, stage-classified, size-specific densities $s_i(z,\theta,t)$ and associated fishing-mortality rates. The spatial distribution of annual catch, $C(\theta)$, was computed by integration of $c(\theta,t)$ in time over each year. Total annual catch, C, was then computed by integration of $C(\theta)$ over the one-dimensional boundary.

Finally, we created 28 marine-reserve configurations (Fig. 8) using a multifactorial combination of four locations and seven sizes. The four reserve locations were chosen to be evenly distributed around the sound (roughly in its SE, NE, NW, and SW quadrants). We considered seven reserve sizes covering 5–40% of available coastal habitat. At the 40% size, adjacent reserves at different locations partially overlapped. Fishing effort displaced by the reserve was assumed to be evenly redistributed over the remaining coastal boundary region. We modified fishing-mortality rates to reflect the displaced effort by assuming that local rates of fishing mortality were proportional to local rates of effort (see, e.g., Polacheck, 1990). Thus, the nominal rate of fishing mortality in the exploited region, F_{mr}, after creation of a marine reserve with length L_{mr}, was

$$F_{mr} = \frac{F}{\left(1 - \frac{L_{mr}}{L}\right)} \qquad \text{Eq. 1}$$

where F is the rate with no reserve (1.0 yr^{-1} here) and L is the total length of habitable coastline. For each case, the model state from the corresponding exploited case at the beginning of model year 40 was used to initialize the model run. The model was subsequently numerically integrated for 10 yrs. As with all model runs, abundance patterns for each postsettlement stage, larval production, and postlarval settlement were saved at quarterly intervals. As with the exploited cases, total catch was recorded annually.

For each hydrodynamic scenario, we thus generated a no-exploitation/no-reserve case, an exploitation/no-reserve case, and 28 exploitation-with-reserve cases. Starting from identical conditions (model year 30), the no-exploitation/no-reserve case reflects the state of the population under

pristine conditions, the exploitation/no-reserve case reflects the state of the population and fishery after 20 yrs of heavy exploitation, and the exploitation-with-reserve cases reflect the state of the population and fishery after 10 yrs of heavy exploitation followed by 10 yrs of continued heavy exploitation but with a refuge area. We evaluate reserve function by comparing annual larval production and catch rates for the final year of each simulation.

Results

No Exploitation, No Reserve.—Despite our use of identical parameter values for natural mortality, growth, dispersal, and reproduction, each hydrodynamic scenario imposed a dramatically different spatial pattern of settlement and larval production along the coastline (Fig. 9). When larvae were dispersed through turbulent diffusion alone (D1), settlement along the coastline was approximately constant for spatial scales greater than 10 km (Fig. 9A). When advection by hydrodynamic currents was included (AD1 and AD2), settlement was spatially segregated and variable: AD1 exhibited three to five principal peaks in settlement ~50–150 km apart (Fig. 9B), and AD2 showed a single peak ~50 km from the mouth of Exuma Sound (Fig. 9C). The spatial pattern of larval production reflected, to a large degree, the spatial pattern of settlement for each hydrodynamic scenario (Fig. 9), but density-dependent mortality in the early benthic stages and dispersal in the later stages modified the pattern of larval production from that of settlement, smearing out the pattern at settlement and reducing variability. For the advective current scenarios in which settlement was focused, postsettlement dispersal allowed larval production to occur over a somewhat larger expanse of the coastline than that at which settlement occurred (Fig. 9B,C).

Annual rates of total larval production (LP_T) and settlement (S_T) varied by an order of magnitude among the three hydrodynamic scenarios (Table 4). Total settlement was highest for D1, lowest for AD2, and intermediate for AD1; the ordering was identical for larval production. The ratio LP_T/S_T, however, differed among the hydrodynamic scenarios (Table 4), reflecting higher postsettlement mortality due to density dependence in the hydrodynamic cases where advection focused settlement patterns in particular regions (i.e., Fig. 9C for AD2).

Exploitation, No reserves.—The relative effect of exploitation on larval production and settlement depended on hydrodynamic scenario. The high exploitation rate ($F = 1.0$ yr^{-1}) considered in this study led to dramatically lower total settlement and larval production than in the unexploited cases, for all three hydrodynamic scenarios (Table 5). The largest differences occurred for D1 (~3 orders of magnitude), the smallest for AD2 (~2 orders of magnitude). Exploitation increased total mortality rates, but relative changes in larval production and settlement were smaller under the advection-diffusion scenarios than under the diffusion-only scenario because relative increases in mortality rates were smaller under the advection-diffusion scenarios, reflecting higher local density-depen-

Table 4. Total annual larval production (LP_T) and settlement (S_T) rates by hydrodynamic scenario for no exploitation, no reserve. Rates are individuals yr^{-1}.

Hydrodynamic scenario	LP_T	S_T	LP_T/S_T
D1	2.1×10^{11}	8.8×10^{6}	2.3×10^{4}
AD1	7.6×10^{10}	4.7×10^{6}	1.6×10^{4}
AD2	8.9×10^{9}	6.1×10^{5}	1.5×10^{4}

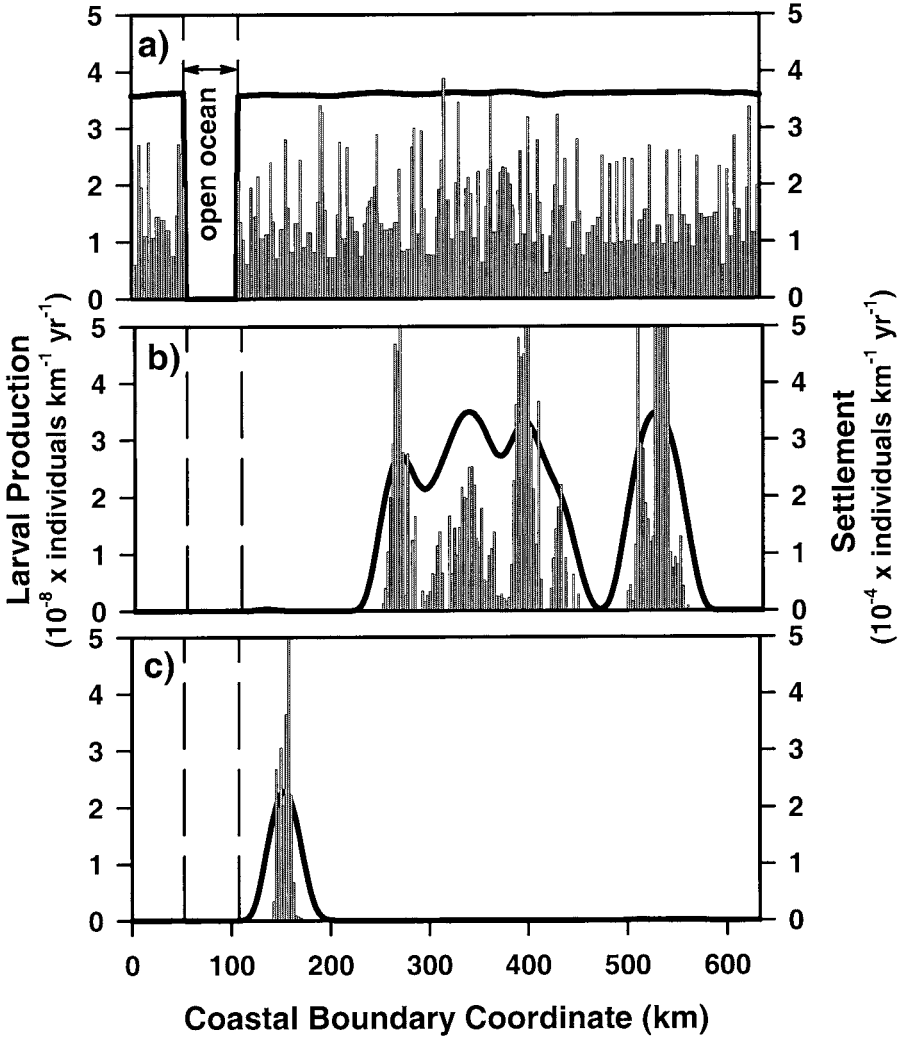

Figure 9. Spatial distribution in model year 50 of annual settlement (grey fill) and larval production (solid line) for the no-exploitation, no-reserve case under each hydrodynamic scenario: (A) D1, (B) AD1, (C) AD2.

Table 5. Total annual larval production (LP_T) and settlement (S_T) rates by hydrodynamic scenario for exploitation (F = 1.0 yr^{-1}) with no reserve. Rates are individuals yr^{-1}.

Hydrodynamic scenario	LP_T	S_T	LP_T/S_T
D1	2.5×10^8	1.1×10^4	2.3×10^4
AD1	6.2×10^8	4.4×10^4	1.4×10^4
AD2	1.3×10^8	9.9×10^3	1.3×10^4

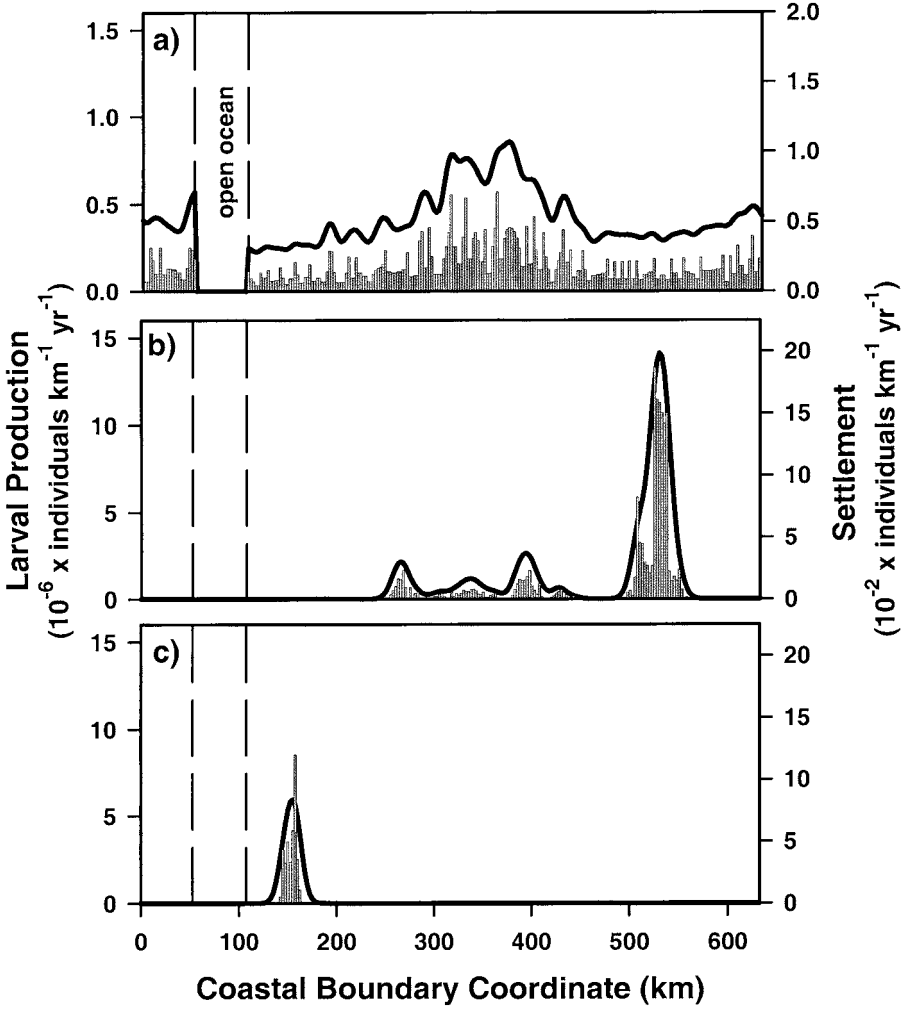

Figure 10. Spatial distribution in model year 50 of annual settlement (grey fill) and larval production (solid line) for the exploitation-only, no-reserve case under each hydrodynamic scenario: (A) D1, (B) AD1, (C) AD2.

dent mortality, as a result of advection-focused settlement patterns, in the corresponding unexploited cases.

In addition, the spatial patterns of larval production and settlement were substantially altered under two hydrodynamic scenarios (D1, AD1; Fig. 10A,B) but not under the third (AD2; Fig. 10C). For all hydrodynamic scenarios, the spatial concordance among settlement, adult density, and larval production increased over the unexploited cases. Under diffusion alone (D1), the constriction and termination of the sound at its northwestern end (Fig. 1), coupled with vastly reduced larval production, actually increased relative local retention and led to higher settlement and subsequent adult abundance there than in other coastal regions. Under AD1, survival rates were spatially structured in the unexploited case because of density-dependent mortality during the early benthic stages—survival rates were lowest where settlement was highest, higher where settlement was low—but

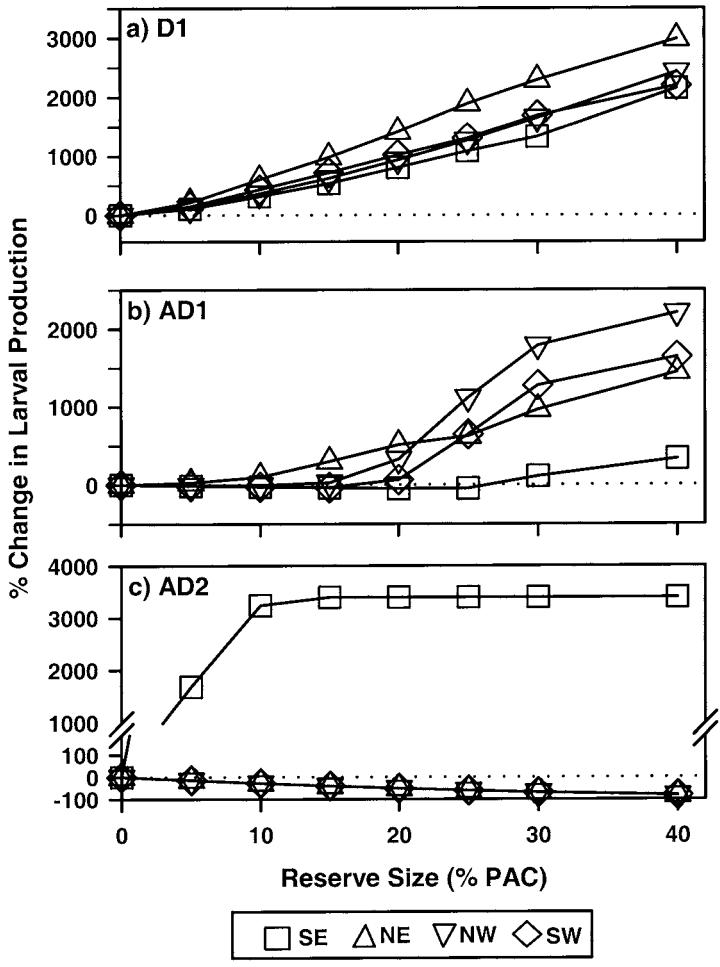

Figure 11. Effect of reserve configuration (size expressed as PAC, see text) and hydrodynamic conditions on larval production for the exploitation-with-reserve cases. The change in larval production was calculated as $(LP_{MR}/LP_{E}-1) \times 100(\%)$, where LP_{MR} represents the total larval production in model year 50 for the exploitation-with-reserve case and LP_{E} represents the total larval production in model year 50 for the corresponding exploitation, no-reserve case. Model results are plotted as functions of reserve size (PAC) for each reserve location: SE (□), NE (Δ), NW (∇), and SW (◊). Results for each hydrodynamic scenario are graphed separately: (A) D1, (B) AD1, (C) AD2.

high exploitation rates resulted in reduced settlement rates overall. Consequently, the effect of spatially heterogeneous, density-dependent mortality was reduced, and the pattern of local abundance more closely reflected that of settlement. For all three scenarios, high exploitation rates reduced postsettlement dispersal, potentially altering connectivity among regions within the sound.

Exploitation with Reserves.—When reserve size was expressed in terms of the fraction of the coastline covered by the reserve (the protected area coverage, PAC), the response of larval production to reserve configuration was not a function of reserve size alone but was also sensitive to reserve location and hydrodynamic scenario (Fig. 11). In D1, larval production increased rapidly with reserve size at all locations (Fig. 11A). In

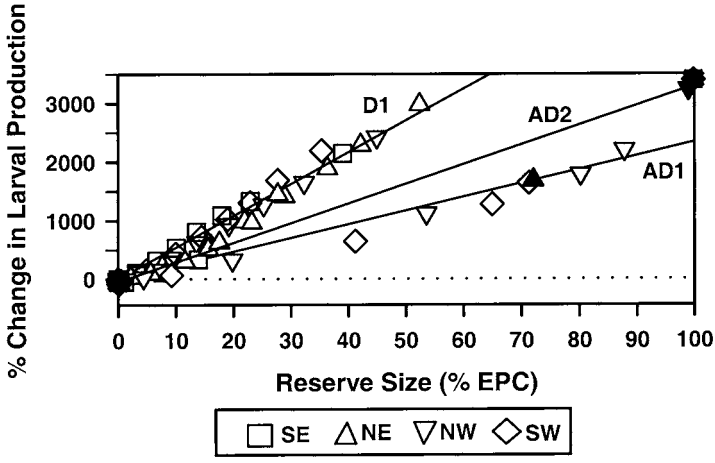

Figure 12. Effect of reserve configuration (size expressed as EPC, see text) and hydrodynamic conditions on larval production for the exploitation-with-reserve cases. The change in total larval production was calculated as for Figure 11. Model results are plotted as functions of reserve size (EPC) and shaded differently for each hydrodynamic scenario (D1, no shading; AD1, grey shading; AD2, black). A linear fit to the results is also shown for each hydrodynamic scenario. Reserve location is indicated by different symbols: SE (□), NE (Δ), NW (▽), and SW (◊).

contrast, larval production under AD1 was reduced from that of the no-reserve case for several reserve locations when reserve size was small. When reserves were larger than 20%, however, larval production increased rapidly with size for all locations, as under D1 (Fig. 11B). In addition, variation in response among reserve locations at the same reserve size was greater for AD1 than for D1. In AD2, larval production responded positively to reserve size at only one location (SE), where larval production increased rapidly with reserve size, reaching an asymptote at a reserve size near 10% (Fig. 11C). For the other three reserve locations, larval production decreased with reserve size under AD2.

The dependence of the larval-production response on reserve location for a given hydrodynamic scenario disappears if reserve size is expressed in terms of the exploited population coverage (EPC) rather than PAC. We define EPC as the fraction of the exploited population (prior to reserve creation) that settled in the reserve area and would be protected under a given reserve configuration. Thus, EPC incorporates actual settlement rates in a reserve location, whereas PAC does not. Because the exploited populations, particularly under AD1 and AD2, exhibit substantial spatial heterogeneity (Fig. 10B,C), PAC and EPC are not equivalent. For all three hydrodynamic scenarios, EPC provides a simpler description than PAC for the response of larval production to reserve creation when EPC is larger than 1–2% (Fig. 12). When EPC is smaller than 1%, larval production is reduced from that in the case with no reserve. In contrast, when EPC is greater than 2%, larval production increases linearly with EPC for each hydrodynamic scenario. The effect of reserve location, independent of EPC, on larval production is relatively small, but using EPC does not remove the effect of hydrodynamic scenario. The slopes for linear regressions of larval production against EPC are substantially different for the three scenarios: the slope for D1 is more than twice that for AD1 (Fig. 12).

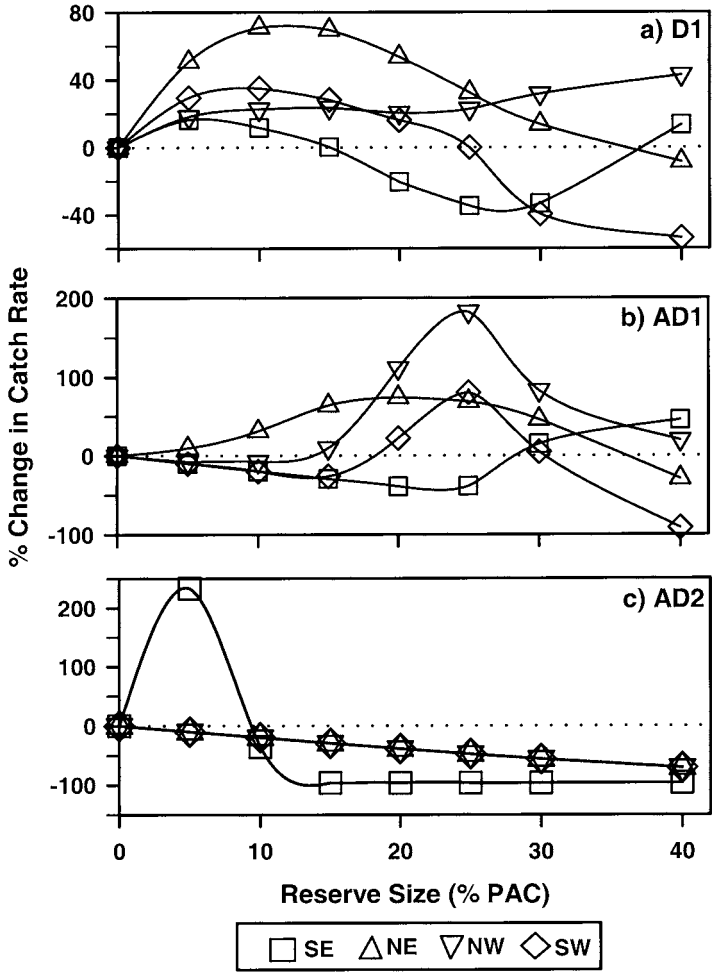

Figure 13. Effect of reserve configuration on catch (size expressed as PAC, see text) for the exploitation-with-reserve cases. The change in catch was calculated as $(C_{MR}/C_E - 1) \times 100(\%)$, where C_{MR} represents the total catch in model year 50 for the exploitation-with-reserve case and C_E represents the total catch in model year 50 for the corresponding exploitation, no-reserve case. Model results are plotted as functions of reserve size (PAC) for each reserve location: SE (□), NE (Δ), NW (∇), and SW (◊). Results are graphed separately for each hydrodynamic scenario: (A) D1, (B) AD1, (C) AD2.

Total annual catch varied dramatically with reserve size (PAC), location, and hydrodynamic scenario (Fig. 13), indicative of a strong three-way interaction among these factors. Optimal combinations of reserve site and size increased catch rates by 75–200%, whereas some suboptimal combinations decreased catch in some cases. For each hydrodynamic scenario, at least one combination of reserve size and location increased catch, but the optimal reserve size and location differed for each hydrodynamic scenario. Furthermore, any apparent functional dependence (e.g., parabolic, Fig. 13) of catch on reserve size varied with reserve location both within and between hydrodynamic scenarios.

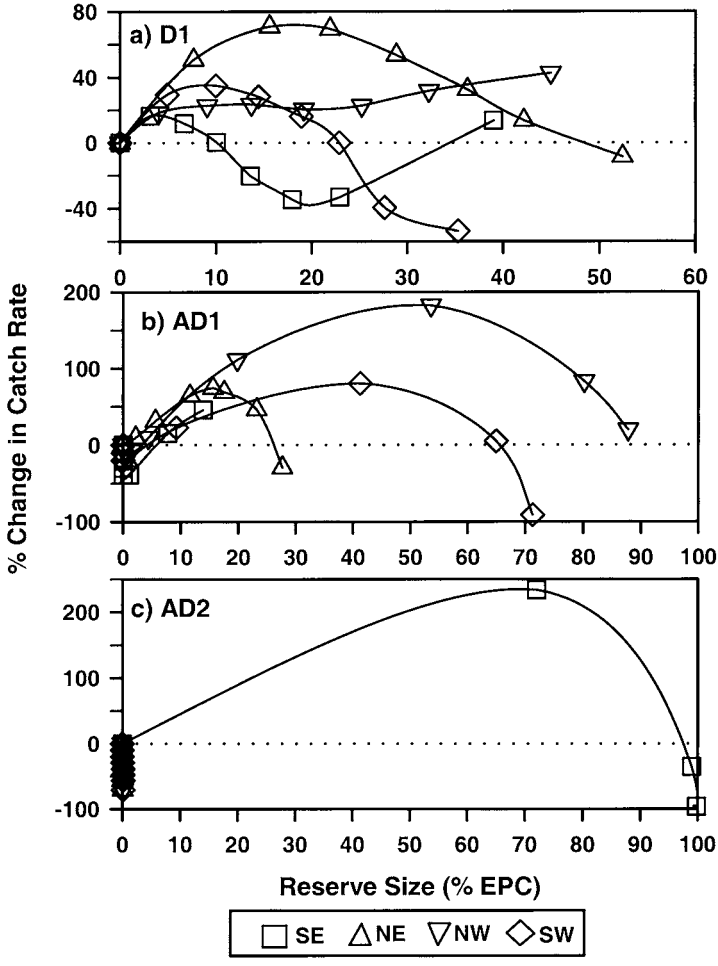

Figure 14. Effect of reserve configuration on catch (size expressed as EPC, see text) for the exploitation-with-reserve cases. The change in total catch was calculated as for Figure 13. Model results are plotted as functions of reserve size (EPC) for each reserve location: SE (□), NE (Δ), NW (∇), and SW (◊). Results are graphed separately for each hydrodynamic scenario: (A) D1, (B) AD1, (C) AD2.

Expressing catch in terms of EPC did not remove the effect of reserve location (Fig. 14). At small EPC (<1%), catch was lower than that in the case with no reserve. For the two advection-diffusion scenarios, catch rate exhibited a somewhat parabolic dependence on EPC for each reserve location—first increasing to a maximum positive value then decreasing and turning negative—as EPC increased (Fig. 14B,C), but the shape of the parabola (e.g., location of the maximum) varied with reserve location. In the diffusion-only scenario, using EPC did not reduce the complexity of the response for catch (Fig. 14A); catch remained a function of reserve size, location, and hydrodynamic scenario even when reserve size was expressed as EPC.

Discussion

Our model results indicate that marine reserves can be effective tools for management of heavily exploited, benthic marine species like the Caribbean spiny lobster, though their efficacy is determined by spatial aspects of population dynamics. Many configurations of reserve size and location yielded both higher catch and higher larval production than cases with no reserve, illustrating that enhancement of yield and the spawning stock can be achieved simultaneously. In contrast, certain reserve configurations caused simultaneously decreased catches and decreased larval production. For each of the three hydrodynamic scenarios considered, one 'optimal' reserve configuration simultaneously maximized catch and increased larval production, but both the size and location of optimal reserves were unique to each hydrodynamic scenario. In our model, each hydrodynamic scenario altered the pattern of connectivity among coastal sites via larval dispersal and postlarval settlement. Our results therefore further suggest that reserve effects are not functions of size alone but also depend on reserve location and the pattern of connectivity among sites. Although not surprising (Carr and Reed, 1993), this aspect of determining 'optimal' marine reserves has not been addressed.

Catch rates (i.e., yield), in particular, responded to reserve size, location, and hydrodynamic scenario in a complex fashion, indicating that the interaction between reserve features and pattern of connectivity is critical. In addition, although larval production responded linearly to the relative fraction of the exploited population protected by a reserve (i.e., EPC) regardless of reserve location, the slope of this relationship differed substantially among hydrodynamic scenarios. Our model results suggest that, (1) under a particular hydrodynamic condition, reserves of similar size (measured as EPC but not as PAC) but at different locations function similarly to increase larval production but do not increase catch rates equivalently; (2) under different hydrodynamic conditions, identical reserve configurations do not function equivalently; and (3) both size and location of 'optimal' reserves differ with hydrodynamic conditions.

Previous theoretical studies of marine reserves (Polacheck, 1990; DeMartini, 1993; Quinn et al., 1993; Attwood and Bennett, 1995; Man et al., 1995) used models based on simple connections among sites. Consequently, reserve performance was characterized by reserve size alone (Polacheck, 1990; DeMartini, 1993; Man et al., 1995) or by reserve size and spacing (Quinn et al., 1993; Attwood and Bennett, 1995). In contrast, our results indicate that the interaction between reserve location and hydrodynamic current pattern, or other factors affecting connectivity among sites, can be complex. It is therefore unlikely that successful designs from one area will 'translate' directly into successful designs for another. Furthermore, no simple 'rule' of reserve design (e.g., 20% of a region) can be generalized across all marine species and ecosystems. For example, significant increases in larval production occurred at reserve sizes of 10–40 % in most cases considered here, depending on hydrodynamic scenario. In a few cases, however, reserves decreased larval production at all reserve sizes. Use of a 20% rule would, in some cases, lead to a false sense of security, thereby endangering—not protecting—exploited stocks.

Predicting the consequences of the interaction between reserve configuration and connectivity pattern is critical to the design of optimally functioning reserves, but prediction requires detailed information not only on life-history characteristics and abundance patterns for the target species but also on hydrodynamic current patterns. For a small number of well-studied species, the requisite information may be available, and spatially explicit

models of the type used here, which integrate life-history characteristics, hydrodynamic patterns for larval dispersal, and spatial patterns of exploitation, may be useful in comparing alternative reserve designs. For most species, however, funding levels and time constraints are unlikely to allow fishery managers to incorporate the required level of detail about connectivity. In addition, the stochastic nature of hydrodynamic patterns and other environmental effects, population processes like recruitment success and interspecific interactions, and the human component of fisheries dictate taking a bet-hedging approach (Lauck et al., 1998) that spreads the risk associated with incomplete information (Lauck et al., 1998; Sladek Nowlis and Roberts, 1999).

We therefore recommend, to paraphrase Dante, abandoning all hope of designing optimal marine reserves—at least in the deterministic sense. An alternative approach to 'optimal' reserve design is to create relatively dense networks of small reserves (Roberts, 1997, 1998) at randomly selected locations such that a substantial fraction of the population (e.g., EPC > 5%) is protected. Multiple small reserves may function more effectively than a single large reserve in a deterministic fashion, particularly for species with sedentary adults and planktonic larvae (Quinn et al., 1993; Attwood and Bennett, 1995), and this strategy also allows one to 'spread the risks' associated with a single reserve. Because edge effects mean that smaller reserves can permit high transfer rates between reserve and exploited areas, and concomitant loss of spawning stock as motile individuals disperse beyond reserve boundaries, the trade-off between reserve size and postsettlement dispersal rates will be an important issue. Finally, the use of traditional conservation tactics (e.g., effort reduction to reduce exploitation rates) may be effective as a supplement or substitute for marine reserves where the efficacy of reserves remains questionable (Lipcius and Crowder, unpubl.).

Acknowledgments

We are extremely grateful to F. Coleman for organizing The Second Mote International Symposium and the associated proceedings, as well as to J. Bohnsack and three anonymous referees for their critical reviews. This investigation was supported by funds from the National Undersea Research Program of the National Oceanic and Atmospheric Administration, the Caribbean Marine Research Center, the National Science Foundation, and the Commonwealth of Virginia. This is contribution No. 2278 from the Virginia Institute of Marine Science.

Literature Cited

Acosta, C. A. 1999. Benthic dispersal of Caribbean spiny lobsters among insular habitats: implications for the conservation of marine species. Cons. Biol. 13: 603–612.

Alcala, A. C. and G. R. Russ. 1990. A direct test of the effects of protective management on abundance and yield of tropical marine resources. J. Cons. Cons. Int. Éxplor. Mer 46: 40–47.

Andree, S. W. 1981. Locomotory activity patterns and food items of benthic postlarval spiny lobsters, *Panulirus argus*. M.S. Thesis, Florida State Univ., Tallahassee. 50 p.

Attwood, C. G. and B. A. Bennett. 1995. Modeling the effects of marine reserves on the recreational shore-fishery of the South-Western Cape, South Africa. S. Afr. J. Mar. Sci. 16: 227–240.

Berrill, M. 1975. Gregarious behavior of juveniles of the spiny lobster, *Panulirus argus* (Crustacea: Decapoda). Bull. Mar. Sci. 25: 515–522.

Bohnsack, J. A., D. E. Harper and D. B. McClellan. 1994. Fisheries trends from Monroe County, Florida. Bull. Mar. Sci. 54: 982–1018.

Booth, J. D. and B. F. Phillips. 1994. Early life history of spiny lobster. Crustaceana 66: 271–294.
Botsford, L. W. 1985. Models of growth. Pages 171–188 *in* A. M. Wenner, ed. Crustacean issues, vol. 3: factors in adult growth. A. A. Balkema, Rotterdam.
Butler, M. J. and W. F. Herrnkind. 1992. Spiny lobster recruitment in south Florida: quantitative experiments and management implications. Proc. Gulf Carib. Fish. Inst. 41: 508–515.
_____ and _____. 1997. A test of recruitment limitation and the potential for artificial enhancement of spiny lobster (*Panulirus argus*) populations in Florida. Can. J. Fish. Aquat. Sci. 54: 452–463.
Calinski, M. D. and W. G. Lyons. 1983. Swimming behavior of the puerulus of the spiny lobster *Panulirus argus* (Latreille, 1804) (Crustacea: Palinuridae). J. Crust. Biol. 3: 329–335.
Carr, M. H. and D. C. Reed. 1993. Conceptual issues relevant to marine harvest refuges: examples from temperate reef fishes. Can. J. Fish. Aquat. Sci. 50: 2019–2028.
Childress, M. J. 1997. Marine reserves and their effects on lobster populations: report from a workshop. Mar. Freshw. Res. 48: 1111–1114.
Cobb, J. S. and J. F. Caddy. 1989. The population biology of decapods. Pages 327–374 *in* J. F. Caddy, ed. Marine invertebrate fisheries: their assessment and management. John Wiley & Sons, New York.
Colin, P. L. 1995. Surface currents in Exuma Sound, Bahamas and adjacent areas with reference to potential larval transport. Bull. Mar. Sci. 56: 48–57.
Davis, G. E. and J. Dodrill. 1980. Marine parks and sanctuaries for spiny lobster fishery management. Proc. Gulf Carib. Fish. Inst. 32: 194–207.
_____ and _____. 1989. Recreational fishery and population dynamics of spiny lobster, *Panulirus argus*, in Florida Bay, Everglades National Park, 1977–1980. Bull. Mar. Sci. 44: 78–88.
DeMartini, E. E. 1993. Modeling the potential of fishery reserves for managing Pacific coral reef fishes. Fish. Bull., U.S. 91: 414–427.
Die, D. J. and R. A. Watson. 1992. A per-recruit simulation model for evaluating spatial closures in an Australian penaeid fishery. Aquat. Living Resour. 5: 145–153.
Doherty, P. J. 1991. Spatial and temporal patterns of recruitment. Pages 261–293 *in* P. F. Sale, ed. The ecology of fishes on coral reefs. Academic Press, San Diego.
_____ and T. Fowler. 1994. An empirical test of recruitment limitation in a coral reef fish. Science 263: 935–939.
Dugan, J. E. and G. E. Davis. 1993. Applications of marine refugia to coastal fisheries management. Can. J. Fish. Aquat. Sci. 50: 2029–2042.
Eckman, J. E. 1996. Closing the larval loop: linking larval ecology to the population dynamics of marine benthic invertebrates. J. Exp. Mar. Biol. Ecol. 200: 207–237.
Eggleston, D. B., R. N. Lipcius, L. S. Marshall, Jr., and S. G. Ratchford. 1998. Spatiotemporal variation in postlarval recruitment of the Caribbean spiny lobster in the central Bahamas: lunar and seasonal periodicity, spatial coherence, and wind forcing. Mar. Ecol. Prog. Ser. 174: 33-49.
_____, _____, D. L. Miller and L. Coba-Cetina. 1990. Shelter scaling regulates survival of juvenile Caribbean spiny lobster *Panulirus argus*. Mar. Ecol. Prog. Ser. 62: 79–88.
_____, _____ and _____. 1992. Artificial shelters and survival of juvenile Caribbean spiny lobster *Panulirus argus*: spatial, habitat, and lobster size effects. Fish. Bull., U.S. 90: 691–702.
Fogarty, M. 1998. Implications of migration and larval interchange in American lobster (*Homarus americanus*) stocks: spatial structure and resilience. Pages 273–283 *in* G. S. Jamieson and A. Campbell, eds. Proc. North Pacific Symp. Invertebrate Stock Assessment and Management. Can. Spec. Publ. Fish. Aquat. Sci. 125.
Forcucci, D., M. J. Butler and J. H. Hunt. 1994. Population dynamics of juvenile Caribbean spiny lobster, *Panulirus argus*, in Florida Bay, Florida. Bull. Mar. Sci. 54: 805–818.

Gaines, S. D. and K. D. Lafferty. 1995. Modeling the dynamics of marine species: the importance of incorporating larval dispersal. Pages 389–412 *in* L. R. McEdward, ed. Ecology of marine invertebrate larvae. CRC Press, Boca Raton, Florida.

Gitschlag, G. R. 1986. Movement of pink shrimp in relation to the Tortugas sanctuary. N. Am. J. Fish. Manage. 6: 328–338.

Guénette, S., T. Lauck and C. Clark. 1998. Marine reserves: from Beverton and Holt to the present. Rev. Fish Biol. Fish. 8: 251–272.

Hastings, A. and L. W. Botsford. 1999. Equivalence in yield from marine reserves and traditional fisheries management. Science 284: 1537–1538.

Herrnkind, W. F. 1980. Spiny lobsters: patterns of movement. Pages 349–407 *in* J. S. Cobb and B. F. Phillips, eds. Biology and management of lobsters, vol. 1: physiology and behavior. Academic Press, New York.

_____. 1983. Movement patterns and orientation. Pages 41–105 *in* F. J. Vernberg and W. B. Vernberg, eds. The biology of Crustacea, vol. 7: behavior and ecology. Academic Press, New York.

_____ and M. J. Butler. 1986. Factors regulating postlarval settlement and juvenile microhabitat use by spiny lobsters, *Panulirus argus*. Mar. Ecol. Prog. Ser. 34: 23–30.

_____, P. Jernakoff and M. J. Butler. 1994. Puerulus and post-puerulus ecology. Pages 213–229 *in* B. F. Phillips, J. S. Cobb and J. Kittaka, eds. Spiny lobster management. Blackwell Science, London.

_____ and R. N. Lipcius. 1989. Habitat use and population biology of Bahamian spiny lobster. Proc. Gulf Carib. Fish. Inst. 39: 265–278.

Hickey, B. M. 1995. Circulation and water properties of Exuma Sound. Unpublished presentation at the Chapman Conference, Amer. Geophys. Union. La Parguera, Puerto Rico.

Holland, D. S. and R. J. Brazee. 1996. Marine reserves for fisheries management. Mar. Resour. Econ. 11: 157–171.

Hunt, J. H. and W. G. Lyons. 1986. Factors affecting growth and maturation of spiny lobsters, *Panulirus argus*, in the Florida Keys. Can. J. Fish. Aquat. Sci. 43: 2243–2247.

Jones, G. 1991. Postrecruitment processes in the ecology of coral reef fish populations: a multifactorial perspective. Pages 294–328 *in* P. F. Sale, ed. The ecology of fishes on coral reefs. Academic Press, San Diego.

Kanciruk, P. and W. Herrnkind. 1978. Mass migration of spiny lobster, *Panulirus argus* (Crustacea: Palinuridae): behavior and environmental correlates. Bull. Mar. Sci. 28: 601–623.

Lauck, T., C. W. Clark, M. Mangel and G. R. Munro. 1998. Implementing the precautionary principle in fisheries management through marine reserves. Ecol. Appl. 8: S72–S78.

Leis, J. M. 1991. The pelagic stage of reef fishes: the larval biology of coral reef fishes. Pages 183–230 *in* P. F. Sale, ed. The ecology of fishes on coral reefs. Academic Press, San Diego.

Lewis, J. B. 1951. The phyllsoma larvae of the spiny lobster, *Panulirus argus*. Bull. Mar. Sci. 1: 89–103.

_____, H. B. Moore and W. Babis. 1952. The postlarval stages of the spiny lobster, *Panulirus argus*. Bull. Mar. Sci. 2: 324–337.

Lipcius, R. N. 1985. Size-dependent timing of reproduction and molting in spiny lobsters and other longlived decapods. Pages 129–148 *in* A. Wenner, ed. Crustacean issues, vol. 3: factors in adult growth. A. A. Balkema, Rotterdam.

_____ and J. S. Cobb. 1994. Ecology and fishery biology of spiny lobsters. Pages 1–30 *in* B. F. Phillips, J. S. Cobb and J. Kittaka, eds. Spiny lobster management. Blackwell Science, London.

_____ and D. B. Eggleston. (in press). Ecology and fishery biology of spiny lobsters. *In* B. F. Phillips and J. Kittaka, eds. Spiny lobsters: fisheries and culture. Blackwell Science, Oxford.

_____ and W. F. Herrnkind. 1987. Control and coordination of reproduction and molting in the spiny lobster *Panulirus argus*. Mar. Biol. 96: 207–214.

_____, W. T. Stockhausen, D. B. Eggleston, L. S. Marshall, Jr., and B. Hickey. 1997. Hydrodynamic decoupling of recruitment, habitat quality and adult abundance in the Caribbean spiny lobster: source-sink dynamics? Mar. Freshw. Res. 48: 807–815.

Little, E. J. 1977. Observations on recruitment of postlarval spiny lobsters, *Panulirus argus*, to the south Florida coast. Fla. Dept. Nat. Resour. Mar. Res. Lab., St. Petersburg, Florida. 35 p.

Lyons, W. G. 1980. The postlarval stage of scyllaridean lobsters. Fisheries (Bethesda) 5(4): 47–49.

Man, A., R. Law and N. V. C. Polunin. 1995. Role of marine reserves in recruitment to reef fisheries: a metapopulation model. Biol. Conserv. 71: 197–204.

Marx, J. M. and W. F. Herrnkind. 1985. Macroalgae (Rhodophyta: *Laurencia* spp.) as habitat for young juvenile spiny lobsters, *Panulirus argus*. Bull. Mar. Sci. 36: 423–431.

Mileikovsky, S. 1971. Types of larval development in marine bottom invertebrates, their distributions and ecological significance: a reevaluation. Mar. Biol. 10: 193–213.

Mota Alves, M. I. and R. C. Bezerra. 1968. Sobre o numero de ovos sa langosta *Panulirus argus* (Latr.). Arq. Estac. Biol. Mar. Univ. Fed. Ceara 8: 33–35.

Munro, J. L. 1974. The biology, ecology, exploitation and management of Caribbean reef fishes: scientific report of the ODA/UNI fisheries ecology research project, 1962–1973, part V. I. The biology, ecology, and bionomics of Caribbean reef fishes: VI. Crustaceans (spiny lobster and crabs). Research Report from the Zoology Department, Univ. West Indies, no. 3, Kingston, Jamaica. 57 p.

Okubo, A. 1980. Diffusion and ecological problems: mathematical models. Springer-Verlag, New York. 254 p.

Phillips, B. F. 1981. The circulation of the southern Indian Ocean and the planktonic life of the western rock lobster. Oceanogr. Mar. Biol. Ann. Rev. 19: 11–39.

_____, J. S. Cobb and R. W. George. 1980. General biology. Pages 1–82 *in* J. S. Cobb and B. F. Phillips, eds. The biology and management of lobsters, vol. 1: physiology and behavior. Academic Press, New York.

Polacheck, T. 1990. Year around closed areas as a management tool. Nat. Resour. Model. 4: 327–354.

Possingham, H. P. and J. Roughgarden. 1990. Spatial population dynamics of a marine organism with a complex life cycle. Ecology 71: 973–985.

Quinn, J. F., S. R. Wing and L. W. Botsford. 1993. Harvest refugia in marine invertebrate fisheries: models and applications to the red sea urchin, *Strongylocentrotus franciscanus*. Am. Zool. 33: 537–550.

Roberts, C. M. 1997. Connectivity and management of Caribbean coral reefs. Science 278: 1454–1457.

_____. 1998. Sources, sinks, and the design of marine reserve networks. Fisheries (Bethesda) 23(7): 16–19.

_____ and N. V. C. Polunin. 1991. Are marine reserves effective in management of reef fisheries? Rev. Fish Biol. Fish. 1: 65–91.

Roughgarden, J., S. Gaines and H. Possingham. 1988. Recruitment dynamics in complex life cycles. Science 241: 1460–1466.

Russ, G. R. and A. C. Alcala. 1996. Do marine reserves export adult fish biomass? Evidence from Apo Island, Central Philippines. Mar. Ecol. Prog. Ser. 132: 1–9.

Sladek Nowlis, J. and C. M. Roberts. 1997. You can have your fish and eat it too: theoretical approaches to marine reserve design. Proc. 8th Int'l. Coral Reef Symp. 2: 1907–1910.

_____ and _____. 1999. Fisheries benefits and optimal design of marine reserves. Fish. Bull., U.S. 97: 604–616.

Smith, K. N. and W. F. Herrnkind. 1992. Predation on juvenile spiny lobsters, *Panulirus argus* (Latr.): influence of size, shelter, and activity period. J. Exp. Mar. Biol. Ecol. 157: 3–18.

Strong, D. R. 1984. Density-vague ecology and liberal population regulation in insects. Pages 313–327 *in* P. W. Price, C. N. Slobodchikoff and W. S. Gaud, eds. A new ecology: novel approaches to interactive systems. John Wiley & Sons, New York.

Thorson, G. 1950. Reproductive and larval ecology of marine bottom invertebrates. Biol. Rev. Camb. Philos. Soc. 25: 1–45.

Tremblay, M. J., J. W. Loder, F. E. Werner, C. E. Naimie, F. E. Page and M. M. Sinclair. 1994. Drift of sea scallop larvae *Placopecten magellanicus* on Georges Bank: a model study of the roles of mean advection, larval behavior and larval origin. Deep-Sea Res. II 41: 7–49.

Yamasaki, A. and A. Kuwahara. 1990. Preserved area to effect recovery of overfished Zuwai crab stocks off Kyoto Prefecture. Pages 575–585 *in* Proc. Int'l. Symp. King and Tanner Crabs, November 28–30, 1989, Anchorage, Alaska, USA. AK-SG-90-04. Alaska Sea Grant College Program, Univ. Alaska Fairbanks, Fairbanks, Alaska.

Yeung, C. and M. F. McGowan. 1991. Differences in inshore-offshore and vertical distribution of phyllosoma larvae of *Panulirus, Scyllarus* and *Scyllarides* in the Florida Keys in May-June, 1989. Bull. Mar. Sci. 49: 699–714.

Address: (W.T.S., R.N.L) *Virginia Institute of Marine Science, College of William & Mary, P.O. Box 1346, Gloucester Point, Virginia 23062; Email <buck@vims.edu>;* (B.M.H) *School of Oceanography, WB-10, University of Washington, Seattle, Washington 98195.*

Appendix: Model Details

Pelagic Model.—The number of individuals in stage i at time t in the age interval $[a,a+da]$ in a small rectangle with area $dxdy$ centered at $[x,y]$ is $L_i(x,y,t,a)dxdyda$.

The equation describing the dynamics of larvae ($i = 0$) or postlarvae ($i = 1$) within the oceanic region is

$$\frac{\partial}{\partial_t} L_i = -\frac{\partial}{\partial_a} L_i - \mu_i L_i - \left\{ \frac{\partial}{\partial_x} J_i^x + \frac{\partial}{\partial_y} J_i^y \right\} \qquad \text{Eq. 2}$$

where μ_i is the local rate of mortality and J_i^x, J_i^y are the x, y components of larval/postlarval flux. The first term on the right represents the local change in density due to aging, the second the loss due to mortality, and the term in braces the net change in local density due to emigration/immigration via active migration, hydrodynamic currents, and turbulent diffusion.

Mortality rates for Caribbean spiny lobster phyllosomata and postlarvae have not been measured, although they are presumably high (Booth and Phillips, 1994). For this study, we set the μ_i to constants—independent of location, time, and age within each stage (Table 1).

The flux components J_i^x, J_i^y are related to density by

$$J_i^x(x,y,t,a) = \left\{ u_i - K \frac{\partial}{\partial_x} \right\} L_i$$
$$J_i^y(x,y,t,a) = \left\{ v_i - K \frac{\partial}{\partial_y} \right\} L_i \qquad \text{Eq. 3}$$

where u_i, v_i are the x, y components of advective velocity and K is the coefficient of eddy diffusion. Spiny lobster phyllosomata have little capacity for horizontal movement (Booth

and Phillips, 1994), so larval dispersal is probably primarily passive (although phyllosomata are capable of vertical movement and may be able to use the differences in current structure at different depths to influence dispersal patterns; Phillips, 1981; Yeung and McGowan, 1991). For this study, we assumed larvae to be passively dispersed; thus, u_0 and v_0 are equal to the local hydrodynamic current components u and v. Because postlarvae, in contrast, actively migrate to settlement areas (Calinski and Lyons, 1983; Booth and Phillips, 1994), we expressed the deterministic part of postlarval dispersal as the sum of hydrodynamic current velocity and an active dispersal velocity, $u_1 = u + u_{pl}$ and $v_1 = v + v_{pl}$, where u_{pl}, v_{pl} represent the local components of active migration. We assumed that postlarvae sense and orient to the closest suitable settlement habitat and that the effective migration rate (i.e., that over a tidal cycle) was higher near the coast, where postlarvae can sink and attach to the bottom during adverse currents (Calinski and Lyons, 1983), than further offshore (Table 1).

The pelagic model is completed by two sets of mathematical boundary conditions. The first set is at age 0 for each pelagic stage. Larvae are produced only along the coastal portion of the spatial boundary, so $L_0(x,y,t,a = 0) = 0$ for all x,y not on the boundary. The local rate of production on the boundary is determined in the reproduction model (see below). If we let $R(x,y,t)$ represent the local rate of larval production (per unit distance along the coastline) at x,y on the spatial boundary and let η^x,η^y represent the direction cosines of a vector pointing directly offshore at the same location, the components of the local flux of age-0 larvae into the offshore region are given by

$$J_0^x\left(x,y,t,a=0\right) = R\left(x,y,t\right)\eta^x\left(x,y\right)$$
$$J_0^y\left(x,y,t,a=0\right) = R\left(x,y,t\right)\eta^y\left(x,y\right) \qquad \text{Eq. 4}$$

Metamorphosis to the postlarval stage may be environmentally cued in late-stage phyllosomata by contact with the seafloor or lower-salinity water over the continental shelf (Booth and Phillips, 1994). However, because it results in a major simplification to the model structure, we assume that the duration of the larval stage is fixed (a_{pl}, Table 1) and that metamorphosis to the postlarval stage occurs wherever a_{pl} is reached. As a result, the age-0 boundary condition for the postlarval stage is simply that the local density of age-0 postlarvae equals the local density of age a_{pl} larvae.

The second set of mathematical boundary conditions concerns behavior at the spatial boundary. Because we do not consider immigration from beyond the modeled geographic region, the flux of $a > 0$ larvae, and all postlarvae, across the spatial boundary can only be directed 'outside' the oceanic region, i.e., onto the coast or beyond the deep-water boundaries. Further, actual transport across the boundary may be less than the potential maximum flux because of the stage-specific 'leakiness', $\omega_i(x,y)$, of the boundary. For this study, we assumed that larvae were not swept into coastal areas ($\omega_0 = 0$ along the coastal portion of the boundary) and that transport across deep-water boundaries occurred at 50% of the maximum possible rate ($\omega_0 = 0.5$). Conversely, postlarvae were not lost at deep-water boundaries ($\omega_1 = 0$) but invaded coastal habitats at the maximum possible rate ($\omega_1 = 1$).

Larval and postlarval fluxes across the spatial boundary result in corresponding decreases in density within the pelagic model, but the age-integrated postlarval flux across

coastal portions of the boundary determines the local rate of settlement, S_{pl}. Consequently, postlarvae that cross the coastal boundary represent a loss within the pelagic model but a gain within the benthic model.

BENTHIC MODEL.—We characterize within-stage density by size rather than age because demographic rates for spiny lobster are more typically characterized by size than age (Cobb and Caddy, 1989). For small increments dz in size and distance $d\theta$ along the coast, $s_i(z,\theta,t)d\theta dz$ is the number of benthic individuals in stage i in the size range $[z,z+dz]$ occupying the coastline from $[\theta,\theta+d\theta]$ at time t.

The dynamics of N postsettlement life-history stages along the coast are described by the following set of N coupled partial differential equations:

$$\frac{\partial s_i}{\partial_t} = -\mu_i s_i + \sum_{j=1}^{N} \tau_{ij} s_j - \sum_{j=1}^{N} \tau_{ji} s_i - \frac{\partial}{\partial_z}\left\{g_i s_i\right\} - \frac{\partial}{\partial\theta} J_i + S_i \qquad i = 1 \ldots N \qquad \text{Eq. 5}$$

where μ_i is the instantaneous rate of mortality, τ_{ij} is the rate at which individuals progress from stage j to i, g_i is the instantaneous rate of growth, J_i is the flux of individuals dispersing along the coastline, and S_i is a source term representing influx from outside the model (e.g., settlement). The functions μ_i, τ_{ij}, g_i, and J_i are stage-specific and may also be functions of z, θ, and t. The terms on the right-hand side of Eq. 5 represent (1) losses due to mortality, (2) gains from individuals progressing from the jth to the ith stage, (3) losses from individuals progressing from the ith to the jth stage, (4) losses and gains due to growth of individuals within a stage, (5) losses and gains due to movement of individuals along the coast, and (6) gains from settlement.

Boundary conditions for Eq. 5 take different forms depending on whether the boundary is in space (θ) or in size (z). We do not consider dispersal through deep-water sections of the one-dimensional boundary, so the dispersal flux J_i is required to be zero at intersections of coastal and deep-water portions of the boundary. Similarly, we set zero flux conditions on growth at the minimum and maximum sizes within each life-history stage

$$\left\{g_i\left(z,\theta,t\right)s_i\left(z,\theta,t\right)\right\}\Big|_{z_i^{min}} = \left\{g_i\left(z,\theta,t\right)s_i\left(z,\theta,t\right)\right\}\Big|_{z_i^{max}} = 0 \qquad \text{Eq. 6}$$

because the transition from one stage to the next occurs over a range of sizes. Individuals reaching the maximum size in each life-history stage cease growth until they undergo transition to the next life-history stage.

To incorporate density-dependent processes into the model formulation in a consistent fashion, we use a nondimensional *normalized life-history-stage density* $\zeta_i(\theta,t)$, expressed as

$$\zeta_i\left(\theta,t\right) = \frac{\sum_j c_{ij}\left\{\int dz\, s_j\left(z,\theta,t\right)\right\}}{\Psi_i\left(\theta,t\right)} \qquad \text{Eq. 7}$$

where the c_{ij} are coefficients which characterize the additional effect of life-history stage j on i and $\psi_i(\theta,t)$ is an auxiliary measure of habitat quality or suitability, the *stage-classified index of habitat suitability*. Essentially, $\psi_i(\theta,t)$ represents a measure of the carrying capacity of the local environment for animals in stage i and is an input to the model. In developing Eq. 7, we assume that density-dependent effects are independent of the size structure within each stage and depend only on local stage densities.

For the Caribbean spiny lobster, the benthic model encompasses five postsettlement life-history divisions: algal-phase juvenile, postalgal-phase juvenile, subadult juvenile, adult male, and adult female. Each constitutes a life-history stage within the context of the benthic model. We divided the adult stage into sex-specific components because both adult growth rates (see, e.g., Herrnkind and Lipcius, 1989) and exploitation patterns may be sex-specific, but we chose to use identical life-history parameters for the two sexes in this study.

Within the context of the model, size refers to carapace length (CL). Modeled life-history stages range in size from 6 to 150 mm carapace length (CL, Table 2), although a small fraction of lobsters reach greater size in Exuma Sound (Herrnkind and Lipcius, 1989; Lipcius and Stockhausen, unpubl.).

Different postsettlement life-history stages use different benthic habitats (Herrnkind and Lipcius, 1989; Butler and Herrnkind, 1997), so except for the adult stages, we assumed that density effects within each model stage were independent of the local density of the other stages (in Eq. 7, $c_{ij} = 0$ if $i \neq j$; $c_{ij} = 1$ otherwise). For the two adult stages, we assumed the effective density was the sum of the two densities (in Eq. 7, $c_{ij} = 1$ if $i = 4,5$ and $j = 4,5$; $c_{ij} = 0$ otherwise).

For this study, we also chose to ignore explicit spatial and temporal variability in demographic rates (other than fishing mortality) and in habitat suitability. Demographic rates could vary in space and time because of local changes in density but were otherwise homogeneous in space and time. In addition, we used a set of constants for the habitat index, $\psi_i(\theta,t)$. The selected values (Table 2) reflect an apparent limitation of settlement habitat in portions of Exuma Sound (Lipcius et al., 1997) as well as an assumed decrease in habitat availability with size.

We decomposed the total rate of mortality, $\mu_i(z,\theta,t)$, into additive components associated with fishing ($\mu_i^f(z,\theta,t)$, 'fishing mortality') and other sources ($\mu_i^n(z,\theta,t)$, 'natural mortality'). We expressed the instantaneous rate of fishing mortality as

$$\mu_i^f(z,\theta,t) = \begin{cases} F_i\varphi(\theta) & t^{start} \geq t \geq t^{end}, z \geq z_i^f \\ 0 & otherwise \end{cases} \qquad \text{Eq. 8}$$

where the parameter F_i specifies the nominal level of fishing mortality, z_i^f is the minimum size vulnerable to the fishery, and t^{start} and t^{end} specify the beginning and ending of the fishing season, respectively. The function $\varphi(\theta)$ controls the spatial pattern of effort and determines the configuration of different reserve scenarios. In this formulation, the spatial allocation of fishing effort is independent of patterns of abundance.

Several studies have determined relative mortality of Caribbean spiny lobster in experimental treatments in the field (e.g., Eggleston et al., 1990, 1992; Butler and Herrnkind, 1997), but few studies have estimated absolute rates (e.g., Munro, 1974) and none has done so within Exuma Sound. In Exuma Sound, lack of appropriately scaled shelter may

be an important factor in density-dependent mortality rates (Lipcius et al., 1997), but density dependence is likely only at high densities, after most available shelters are occupied. We therefore modeled the instantaneous rate of natural mortality using the piecewise linear expression

$$\mu_i^n(z,\theta,t) = \mu_i^n(z,\zeta_i) = \begin{cases} c_{i1} & \zeta < c_{i3} \\ c_{i1}\left(1 + c_{i2}\left[\zeta_i - c_{i3}\right]\right) & \zeta \geq c_{i3} \end{cases} \qquad \text{Eq. 9}$$

where the c_{ij} are stage-specific model parameters (Table 2) and $\zeta_i(\theta,t)$ is the normalized stage-specific local density. Local rates of natural mortality are density independent when density is low ($\zeta_i < c_{i3}$) but increase linearly with density when density is high. Because absolute rates have not been measured, we chose parameter values (Table 2) that gave reasonable survival probabilities (Fig. 5; see Butler and Herrnkind, 1997).

We selected a simple, but otherwise arbitrary, functional form for the rate of transition between life-history stages, $\tau_{i,j}(z,\theta,t)$. The rate at which individuals change from stage *j* to stage *i* is

$$\tau_{i,j}(z,\theta,t) = \tau_{i,j}(z) = \begin{cases} 0 & z < z_i^{min} \\ c_{ij1}\left\{1 - e^{-c_{ij2}\left(z - z_i^{min}\right)}\right\} & z \geq z_i^{min} \end{cases} \qquad \text{Eq.10}$$

where the c_{ijk} are stage-specific model coefficients and z_i^{min} is the minimum size at which transitions to later stages occur. In this formulation, the rate of transition is density independent. The coefficients c_{ij1} represent the asymptotic transition rate from stage *j* to stage *i*. The coefficient c_{ij2} governs the rate of increase of $\tau_{i,j}(z,\theta,t)$ with individual size. The parameter values we selected (Table 2) yield reasonable intervals for transition from one stage to the next.

The Gompertz-type function used to express growth rates within a stage was

$$g_i = \alpha_i z \ln\left[\frac{\beta_i}{z}\right] \qquad \text{Eq. 11}$$

Here, α_i controls initial rate of growth and β_i controls the asymptotic size. We chose to ignore density-dependent effects. Stage-specific growth parameters were selected (Table 2) so that mean stage durations were consistent with Butler and Herrnkind (1997). The resulting growth curve (Fig. 5) is reasonably consistent with results from other studies, particularly given the variability in reported growth rates among previous studies (Davis and Dodrill, 1980, 1989; Hunt and Lyons, 1986; Forcucci et al., 1994). As previously noted, growth-rate parameters for adult males and females are identical (Table 2).

Of the postsettlement stages, only subadults and adults disperse over significant distances (Herrnkind, 1980, 1983; Herrnkind and Butler, 1986). We described alongshore

flux, $J_i(z,\theta,t)$, as a one-dimensional diffusion process with a density-dependent diffusion coefficient:

$$J_i(z,\theta,t) = J_i(s_i,\zeta_i) = -\frac{\partial}{\partial x}\left\{\kappa_i(\zeta_i)s_i\right\} \quad \text{Eq. 12}$$

where s_i is the stage-classified, size-dependent local density, $\zeta_i(\theta,t)$ is the normalized stage density, and κ_i is a stage-specific, density-dependent diffusion coefficient defined as

$$\kappa_i(\zeta_i) = c_{il}\left[1 + c_{i2}\frac{\zeta_i}{c_{i3}+\zeta_i}\right] \quad \text{Eq. 13}$$

In the latter equation, the c_{ij} are stage-specific model parameters. The functional form chosen for J_i in Eq. 12 is appropriate when the direction of movement of individuals is locally unbiased, whereas the rate depends only on conditions at the point of departure (Okubo, 1980). The functional form for the diffusion coefficient κ_i allows postsettlement dispersal to be a combination of density-independent and density-dependent effects. We selected parameter values that reflect the generally more sedentary nature of adult spiny lobster than of subadults.

Finally, the benthic model source term, $S_i(z,\theta,t)dzd\theta$, represents the influx of individuals at time t from beyond the model domain into the size increment $[z,\ z+dz]$ within the coastal region $[\theta,\ \theta+d\theta]$. For this study, we did not consider immigration from outside Exuma Sound. Thus, the only influx is from settlement of postlarvae (and subsequent metamorphosis into algal phase juveniles), S_{pl}. Although postlarvae in Exuma Sound range from 4 to 7 mm CL (Lipcius and Stockhausen, unpublished), we chose, for simplicity, to model all postlarvae as metamorphosing into algal-phase juveniles in the size interval 6–7 mm CL. The source term is therefore

$$S_i(z,\theta,t) = \begin{cases} S_{pl}(\theta,t) & 6 \le z < 7,\ i=1 \\ 0 & otherwise \end{cases} \quad \text{Eq. 14}$$

where $i = 1$ refers to the algal-phase juvenile stage.

Reproduction Model.—The rate at which larvae are produced locally, $R(\theta,t)$, is expressed as:

$$R(\theta,t) = \sum_i \int dz\ r_i(t)m_i(z)\mathcal{F}_i(z)s_i(z,\theta,t) \quad \text{Eq. 15}$$

where r_i is the temporal spawning pattern for stage i individuals, m_i is the fraction of stage i individuals that are mature at size z, and $\mathcal{F}_i$ is individual fecundity. Local production of larvae provides the larval-stage age-0 boundary condition (Eq. 4) for the pelagic model and completes the full life-history model.

In Exuma Sound, peak reproductive activity occurs in spring. The incidence of females occupying offshore reefs that carry fertilized egg masses reaches 80% in June, then declines quickly toward autumn (Herrnkind and Lipcius, 1989). For simplicity, we chose to ignore a possible secondary spawning peak in the fall (Herrnkind and Lipcius, 1989) and expressed the temporal variation in spawning, r_i, as spatially homogeneous using a truncated normal distribution function:

$$r_i(z,\theta,t) = r_i(t) = \begin{cases} c_1 e^{-\left(\frac{t-c_2}{2c_3}\right)^2} & t^{start} \le t \le t^{end},\ i=5 \\ 0 & otherwise \end{cases} \qquad \text{Eq. 16}$$

The c_j in Equation 16 influence the overall level of spawning activity, the time of peak spawning, and the variability about the peak. The parameters t^{start} and t^{end} indicate the beginning and ending dates of the spawning season, respectively. The parameter values selected reflect 100% spawning of all mature females during the season and peak spawning in the spring (Fig. 6A, Table 3). For this study, we chose to end the spawning season just before the beginning of the fishing season.

The smallest reported egg-bearing female in Exuma Sound was 85 mm CL (Herrnkind and Lipcius, 1989). Percent female maturity increases to 100% by 100 mm CL. For simplicity, we chose to express the maturity function, m_i, as a knife-edge function of size:

$$m_i(z) = \begin{cases} 1 & z \ge z^{min},\ i=5 \\ 0 & otherwise \end{cases} \qquad \text{Eq. 17}$$

where z^{min} reflects the minimum size at maturity (Table 3).

Individual fecundity (i.e., number of eggs in an egg mass) of spiny lobster has been well described by both size-dependent power laws (Mota Alves and Bezerra, 1968; Lipcius et al., 1997) and exponential functions (Lipcius and Stockhausen, unpublished). In Exuma Sound, individual fecundity does not vary spatially (Lipcius et al., 1997). We expressed fecundity, $\mathcal{F}_i$, as an exponential function of size.

$$\mathcal{F}_i(z,\theta,t) = \mathcal{F}_i(z) = \begin{cases} c_1 e^{c_2\left(z-z^{min}\right)} & i=5 \\ 0 & otherwise \end{cases} \qquad \text{Eq. 18}$$

We reanalyzed fecundity data from Exuma Sound (Lipcius et al., 1997) using an exponential model to determine values for the c_j parameters (Fig. 6B, Table 3).